
Masters Theses

Student Theses and Dissertations

Summer 2016

Mitigation of glass weave skew using a combination of low DK spread glass, multi-ply dielectric and routing direction

Kartheek Nalla

Follow this and additional works at: https://scholarsmine.mst.edu/masters_theses



Part of the [Electromagnetics and Photonics Commons](#)

Department:

Recommended Citation

Nalla, Kartheek, "Mitigation of glass weave skew using a combination of low DK spread glass, multi-ply dielectric and routing direction" (2016). *Masters Theses*. 7859.

https://scholarsmine.mst.edu/masters_theses/7859

This thesis is brought to you by Scholars' Mine, a service of the Missouri S&T Library and Learning Resources. This work is protected by U. S. Copyright Law. Unauthorized use including reproduction for redistribution requires the permission of the copyright holder. For more information, please contact scholarsmine@mst.edu.

MITIGATION OF GLASS WEAVE SKEW USING A COMBINATION OF LOW DK
SPREAD GLASS, MULTI-PLY DIELECTRIC AND ROUTING DIRECTION

by

KARTHEEK NALLA

A THESIS

Presented to the Faculty of the Graduate School of the
MISSOURI UNIVERSITY OF SCIENCE AND TECHNOLOGY

In Partial Fulfillment of the Requirements for the Degree

MASTER OF SCIENCE IN ELECTRICAL ENGINEERING

2016

Approved by

Jun Fan, Advisor
David Pommerenke
Victor Khilkevich

© 2016

Kartheek Nalla

All Rights Reserved

ABSTRACT

As the data rates increase into the multi-gigabit range, the bit periods fall in the range of few tens of picoseconds. At above few Gbps, it becomes very important to reduce skew between differential pairs as it can adversely impact the signal eye and thereby increase bit error rate. The goal of this study is to mitigate the skew contributed by woven glass fabric of PCB dielectrics.

The glass weave skew between differential pairs in a PCB occurs due to the difference in dielectric constants (DK) of glass and resin. This thesis aims to mitigate the skew by reducing the effective DK difference experienced by the traces of a differential pair. Several strategies like using low DK glass, spread glass styles with less gaps in the glass fabric, 1-ply and 2-ply dielectrics, routing the traces in warp and fill directions are studied through measurements taken on several test vehicles.

Since the relative location of traces with respect to glass bundles cannot be controlled, it is highly unlikely to capture the worst case skew from measurements on few test vehicles. Full wave simulation model of laminate with fiber weave is employed. A systematic approach using measurements and simulations to mitigate the differential pair skew is presented.

ACKNOWLEDGMENTS

I would like to express my sincere gratitude to my advisor, Dr. Jun Fan for his constant support and guidance throughout my master's program. I am very grateful to him for training me on how to tackle tough situations in research as well as personal life. I thank Dr. Jun Fan for his valuable insights and research ideas which helped me look at research problems in a new perspective. I am particularly grateful to Dr. David Pommerenke as his advices were of immense help. I would like to express my great appreciation to Dr. Victor Khilkevich for his patient support and encouragement. I express my sincere gratitude to Dr. James Drewniak for his mentoring and motivation that he offered. I express my special thanks to Dr. Daryl Beetner for introducing me to the VLSI and ESD concepts. His support in the projects is greatly appreciated. I am grateful to all the faculty of EMC laboratory for sharing their priceless knowledge with me. I thank all my friends at EMC laboratory, Missouri S&T for their advice and help throughout my master's program.

I am very grateful to Mike Sapozhnikov, Amendra Koul, Brian Baek from Cisco Systems Inc. for giving me opportunity to work on this topic and for their constant support and guidance.

I thank all my friends for their support and encouragement. Finally, I thank my family for their unconditional love, emotional support and encouragement throughout my life.

TABLE OF CONTENTS

	Page
ABSTRACT	iii
ACKNOWLEDGMENTS	iv
LIST OF ILLUSTRATIONS	vii
LIST OF TABLES	x
NOMENCLATURE.....	xi
1. INTRODUCTION.....	1
2. FABRICATION PROCESS OF PCB DIELECTRICS.....	2
3. ORIGIN AND IMPACT OF GLASS WEAVE SKEW	6
3.1. ORIGIN OF GLASS WEAVE SKEW	6
3.2. IMPACT OF GLASS WEAVE SKEW	7
3.2.1. S-Parameters.....	7
3.2.2. Eye Diagram	9
4. REVIEW OF SKEW MITIGATION STRATEGIES	11
4.1. TRACE ROTATION	11
4.2. PANEL ROTATION.....	13
4.3. ZIG-ZAG ROUTING.....	13
4.4. USING SPREAD GLASS	14
4.5. USING LOW DK GLASS.....	15
4.6. USING MULTI-PLY DIELECTRICS	16
5. MEASUREMENT OF GLASS WEAVE SKEW.....	17
5.1. DESIGN OF TEST VEHICLES	17
5.1.1. Footprint Via Optimization.....	19
5.1.2. Routing Strategy	23
5.2. MEASUREMENT SETUP.....	26
5.3. RESULTS AND DISCUSSION	29
5.3.1. Microstrip – Pitch A, B, C	30
5.3.2. Stripline – Pitch A, B, C	31
5.3.3. Stripline – Pitch A: Glass X vs. Y	32

5.3.4. Stripline – Pitch C: Glass X vs. Y	33
6. FULL WAVE MODELING OF GLASS WEAVE	35
6.1. MODELING STRIPLINE ON 1-PLY SPREAD GLASS	35
6.2. VALIDATION OF SIMULATION MODEL	40
6.3. RESULTS AND DISCUSSION	44
6.3.1. Microstrip – Pitch A	44
6.3.2. Stripline – Pitch A.....	45
6.3.3. Methodology to Obtain the Worst Case Skew.....	47
7. CONCLUSION AND FUTURE WORK.....	48
BIBLIOGRAPHY.....	49
VITA	51

LIST OF ILLUSTRATIONS

	Page
Figure 2.1. Steps in fabrication of laminates	2
Figure 2.2. Weft and warp. During weaving process (left), after weaving (right)	2
Figure 2.3. Top view of glass styles. 2116 (left), 1078 (center), 1027 (right)	3
Figure 2.4. Cross-section view of glass fabric	3
Figure 3.1. Differential Microstrip. Trace 1 is on glass & trace 2 on resin (left), trace 1 & trace 2 are on both glass and resin	6
Figure 3.2. Differential Stripline. Bundles are aligned(left), not aligned (right)	7
Figure 3.3. Differential pair transmission line	7
Figure 3.4. Measured single-ended and differential insertion loss of diff. pair with big skew	8
Figure 3.5. Measured single-ended phase – S_{13} & S_{24}	9
Figure 3.6. Measured single-ended phase – S_{13} & S_{24} (Zoomed in).....	9
Figure 3.7. Eye of differential signal. At the transmitter (left), at receiver (right)	10
Figure 3.8. Eye of differential signal at the receiver afterpassing through channel with big skew	10
Figure 4.1. Straight trace routing on woven glass (Left), 10° rotated trace (right)	11
Figure 4.2. Traces rotated by 45° . P is on resin & N is on glass (left), P & N on equal amounts of resin and glass (right).....	12
Figure 4.3. ASICs located on same vertical level on board layout	12
Figure 4.4. Rotated panel with respect to trace.....	13
Figure 4.5. Zig-Zag routing between two ASICs.....	14
Figure 4.6. Cross–Section view of 1037 glass. Square glass (left), spread glass (right) ...	14
Figure 4.7. Top view of 1037 glass. Square glass (left), spread glass (right).....	15
Figure 4.8. Stripline on 1-ply glass dielectric (left), 2-ply glass dielectric (right).....	16
Figure 5.1. Stack up of test vehicles	17
Figure 5.2. Footprints on test vehicles. West-East direction (left), North-South direction (right)	19
Figure 5.3. HFSS model of probe launch for microstrip (left), Stripline (right)	20

Figure 5.4. Back drilled signal vias in probe launch for stripline T03	20
Figure 5.5. Return Loss – Probe launch for Top layer	21
Figure 5.6. Return Loss – Probe launch for T03 stripline layer	21
Figure 5.7. Return Loss – Probe launch for T05 stripline layer	22
Figure 5.8. Return Loss – Probe launch for T07 stripline layer	22
Figure 5.9. Return Loss – Probe launch for T09 stripline layer	23
Figure 5.10. Differential pair routing strategy	23
Figure 5.11. Top side of test vehicle	24
Figure 5.12. Bottom side of test vehicle.....	25
Figure 5.13. Measurement setup – PNA and Microprobe station	27
Figure 5.14. Probe landing on DUT. Close up view (left), from microscope (right)	27
Figure 5.15. Probe calibration on CS3-1000 substrate. Short (top left), Open (top right), load (bottom left), thru (bottom right)	28
Figure 5.16. ADS Circuit for TDT from S-Parameters	28
Figure 5.17. TDT from S-Parameters	29
Figure 5.18. Skew on microstrip in West-East routing – Pitch A, B, C.....	30
Figure 5.19. Skew on microstrip in North-South routing – Pitch A, B, C	30
Figure 5.20. Skew on stripline in West-East routing – Pitch A, B, C.....	31
Figure 5.21. Skew on stripline in North-South routing – Pitch A, B, C	31
Figure 5.22. Skew on Pitch A, 1-ply glass style - Glass X vs Y	32
Figure 5.23. Skew on Pitch A, 2-ply glass style - Glass X vs Y	32
Figure 5.24. Skew on Pitch C, 1-ply glass style - Glass X vs Y	33
Figure 5.25. Skew on Pitch C, 2-ply glass style - Glass X vs Y	33
Figure 6.1. Cross-Section of a stripline obtained using SEM	35
Figure 6.2. Full wave model of stripline embedded in glass weave fabric. Top View (Top), Cross-section view (Bottom)	36
Figure 6.3. Full wave model of 411 mil long stripline embedded in glass weave fabric. .	37
Figure 6.4. ADS circuit – Cascading (4 X 102.9 mil)	37
Figure 6.5. Return loss – Full wave vs Cascaded Model.....	38
Figure 6.6. Insertion loss – Full wave vs Cascaded Model.....	38
Figure 6.7. Unwrapped Phase – Full wave vs Cascaded Model	39

Figure 6.8. Unwrapped Phase (S13) – Simulation vs Measurement	40
Figure 6.9. Unwrapped Phase (S24) – Simulation vs Measurement	41
Figure 6.10. Magnitude (S13) – Simulation vs Measurement	42
Figure 6.11. Magnitude (S24) – Simulation vs Measurement	42
Figure 6.12. TDT – Simulation vs Measurement.....	43
Figure 6.13. Full wave model of Microstrip.....	44
Figure 6.14. Microstrip – Pitch A – Skew vs trace location	45
Figure 6.15. Stripline on 1-ply glass.....	45
Figure 6.16. Skew vs location of trace – Pitch A.....	46
Figure 6.17. Methodology to capture the worst case skew on a particular glass.....	467

LIST OF TABLES

	Page
Table 2.1. IPC standard for various glass styles	4
Table 4.1. Dielectric constants of glass and resin	15
Table 6.1 Insertion loss and unwrapped phase @ 19.9 GHz	39
Table 6.2 DK, DF of Glass and Resin from Correlation	40
Table 6.3 Unwrapped phase comparison between simulation and measurement	41
Table 6.4 TDT zero crossing times and skew – Simulation vs Measurement	43
Table 6.5 Bundle dimensions from SEM in fill direction.....	46

NOMENCLATURE

<u>Symbol</u>	<u>Description</u>
DK	Dielectric constant
DF	Loss tangent
c	Velocity of light/EM wave in free space
v	Velocity of EM wave in a medium
UI	Unit interval
ps	picoseconds
PCB	Printed circuit board
TDT	Time domain transmission
DUT	Device under test
PNA	Performance network analyzer
ADS	Advanced design system
Gbps	Giga bits per second
SEM	Scanning electron microscope

1. INTRODUCTION

With ever increasing data rates, signal integrity issues are on the rise. It is crucial to consider all the possible factors that affect the integrity of the transmitted signal. Signal quality will be degraded by many factors like conductor losses, dielectric losses, crosstalk, discontinuities in the transmission paths, etc. In addition to all these factors, skew between the P & N signals of differential pair can degrade the signal eye at multi-gigabit data rates. The skew between the P & N signals of differential pair can be generated at the transmitter itself or in the channel due to asymmetries in lengths of P & N traces or due to glass weave effect.

At high data rates above few Gbps, the skew induced by the inhomogeneity in the dielectric constants of glass and resin becomes significant when compared to the bit duration/unit interval (UI). It is common to use 15 to 20 inch long links on many commercial products. On such long serial data links, skew of 3ps/inch can result in 45 – 60 ps of skew between the P & N signals at the receiver. One study [5] has reported a 10 ps/inch measured skew on some transmission lines. Several methods like rotating traces, zig-zag routing, are proposed by earlier studies to mitigate the skew which may not be applicable to long high speed data links due to the cost and board size constraints. In this study, reduction in skew by using low DK glass, using spread glass styles, 1-ply and 2-ply dielectrics will be evaluated to find a cost effective solution.

Measurements as well as full wave simulations will be used to capture the worst case skew on a particular glass when differential pairs are routed in some particular direction (Warp/Fill). The study focusses only on stripline and microstrip differential pairs.

2. FABRICATION PROCESS OF PCB DIELECTRICS

PCB dielectrics are fabricated using woven glass fabric strengthened by epoxy resin material which makes it inhomogeneous material. Raw glass in marble form is melted in a furnace. Glass yarn is prepared after brushing, sizing and strand forming [8]. The steps in manufacturing laminate are shown in fig. 2.1.

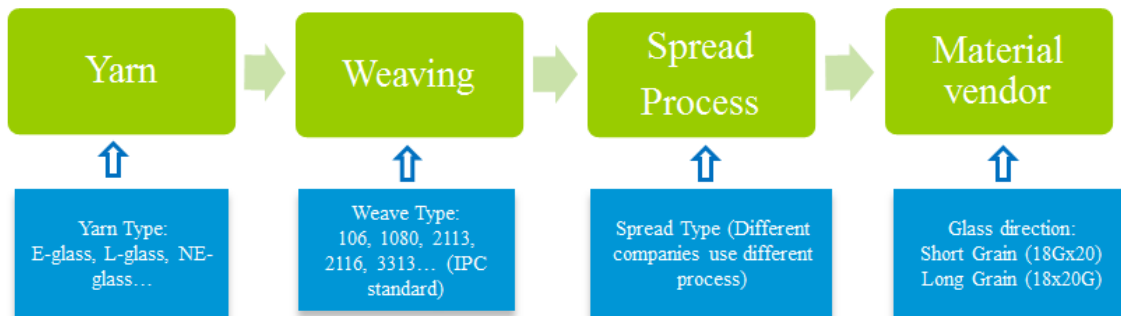


Figure 2.1. Steps in fabrication of laminates

Several glass yarns acquired from the glass yarn manufacturer are grouped into glass bundles. The glass fabric is woven with these bundles. Weaving glass fiber is similar to weaving the garments. Glass bundles are held tight in one direction and glass bundles are woven in the perpendicular direction as shown in fig.2.2.

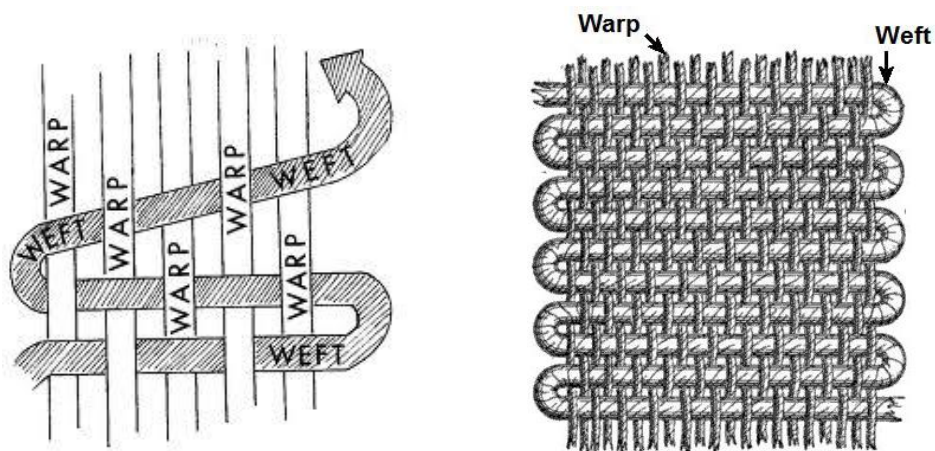


Figure 2.2. Weft and warp. During weaving process (left), after weaving (right)

The direction in which bundles are held tight is called grain direction or warp direction and the direction in which the bundles are woven is called weft or fill direction. Warp (grain) and weft (fill) is shown in fig. 2.2[10]. The glass fabric thus obtained is called square glass fabric. Several glass styles like 106, 1080, 2116, 1078 etc. are defined by the IPC standard as shown in table 2.1. Top view of few glass fabrics is shown in fig. 2.3.

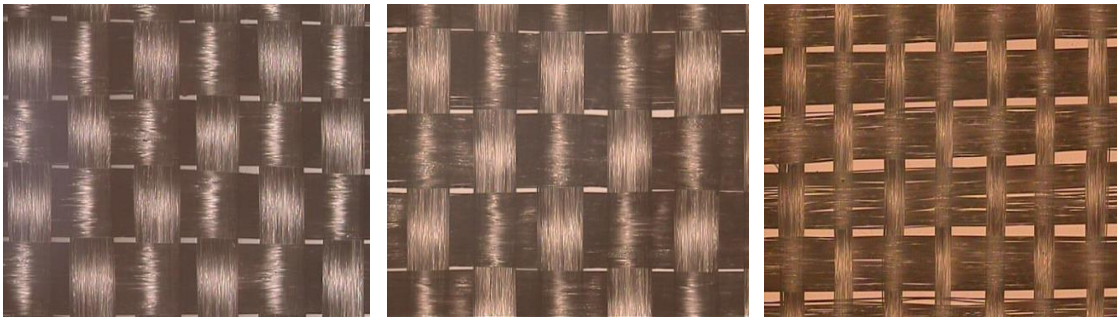


Figure 2.3. Top view of glass styles. 2116 (left), 1078 (center), 1027 (right)

Bundle width, bundle gap, bundle thickness, pitch of glass weave are described in the cross-section view of fiber weave as shown in fig. 2.4. The width, thickness and pitch of the glass bundles are different for each style. The gaps in glass weave can be reduced by spreading the glass bundles. Several spreading companies use different techniques for spreading the glass bundles.

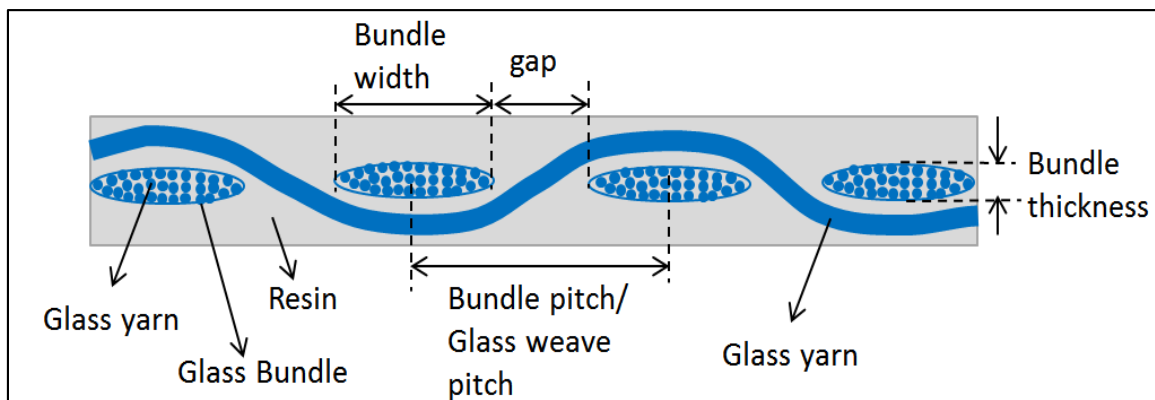


Figure 2.4. Cross-section view of glass fabric

IPC standard defines the number of glass bundles per inch along warp and fill direction. Table 2.1 shows the warp and fill count per inch for several glass styles. Pitch of the glass styles can be calculated from the bundle count per inch. From the table 2.1, 1067 weave style has 70 bundles per inch in warp direction and 73 bundles per inch on fill direction. The pitch of glass bundles in warp and fill can be calculated as

$$\text{Warp pitch} = 1000 \text{ mil}/70 = 14.28 \text{ mil}$$

$$\text{Fill pitch} = 1000 \text{ mil}/58 = 13.69 \text{ mil}$$

Table 2.1. IPC standard for various glass styles

Glass Style	Weave	Warp count	Fill count	Warp yarn	Fill yarn	Fabric thickness Inches	Fabric nominal weight g/m ²
1035	Plain	66	68	ECD 900-1/0	ECD 900-1/0	0.0011	30
1037	Plain	70	73	ECC 1200-1/0	ECC 1200-1/0	0.0011	23
1067	Plain	70	70	ECD 900-1/0	ECD 900-1/0	0.0013	31
1078	Plain	54	54	ECD 450-1/0	ECD 450-1/0	0.0017	48
2116	Plain	60	58	ECD 225-1/0	ECD 225-1/0	0.0038	109
106	Plain	56	56	ECD 900-1/0	ECD 900-1/0	0.0015	25
3313	Plain	61	62	ECDE 300-1/0	ECDE 300-1/0	0.0032	82
2313	Plain	60	64	ECD 225-1/0	ECD 225-1/0	0.0032	81
1080	Plain	60	47	ECD 450-1/0	ECD 450-1/0	0.0025	49

Laminate manufacturers use the woven glass fabric and fill with resin to make large PCB substrates or dielectrics. The gaps between the glass bundles are filled with resin which has lower dielectric constant (DK ~ 3.3) when compared to glass (DK ~ 6) making the dielectrics inhomogeneous. The inhomogeneity is reduced by spreading the glass bundles. The dielectrics thus obtained by hardening the glass weave using epoxy resin are cut into smaller laminates according to the PCB board size requirements of the final product. As per the dielectric manufacturer's capability, panels are either cut in such a way that the longer dimension is along grain or shorter dimension is along grain. 18x24G specifies that the laminate is 24 inches long, 18 inches wide and the long side is the grain direction. Similarly, 18Gx24 indicates that the laminate is short grain. It is important to keep track of grain and fill directions because the width, gap and pitch of glass bundles may be very different in fill and grain direction depending on weave style

and the worst case skew between P & N of differential traces will be different in warp and fill direction due to difference in glass dimensions.

Although the PCB dielectric is inhomogeneous, it is common for the dielectric fabricators to specify the effective DK of the material at a particular frequency. The effective DK is calculated as a weighted average of the volume percentage of the glass, resin and their respective DK's. It is to be noted that density of glass is more than density of resin due to which the percentage of the glass by weight is not same as the percentage of glass by volume.

$$\boldsymbol{\varepsilon}_{r_{eff}} = V_{resin} * \boldsymbol{\varepsilon}_{r_{resin}} + V_{glass} * \boldsymbol{\varepsilon}_{r_{glass}} \quad (1)$$

where $\boldsymbol{\varepsilon}_{r_{eff}}$ is the effective DK of the dielectric, $\boldsymbol{\varepsilon}_{r_{resin}}$ is the DK of resin, $\boldsymbol{\varepsilon}_{r_{glass}}$ is the DK of glass, V_{resin} is the volume percentage of resin, V_{glass} is the volume percentage of glass. The inhomogeneity in dielectrics can be ignored at low frequencies but at higher frequencies in the range of few GHz, the discontinuities become electrically small and the dielectric can no longer be treated as homogeneous material with a bulk dielectric constant [1], [6], [12].

3. ORIGIN AND IMPACT OF GLASS WEAVE SKEW

The electromagnetic waves travel at the speed of light in any given medium. The velocity of EM wave in a medium is given by

$$v = \frac{c}{\sqrt{\epsilon_{r_{eff}}}} \quad (2)$$

where c is the velocity of light in free space, $\epsilon_{r_{eff}}$ is the relative permittivity or dielectric constant of the medium. It is evident from the equation that the wave travels slower in a medium with higher DK than in a medium with lower DK.

3.1. ORIGIN OF GLASS WEAVE SKEW

The dielectric/laminate is a composite formed using glass with higher DK and resin with lower DK, the effective DK seen by the traces will be different based on the relative location of the trace with respect to glass bundle. Cross section of a differential microstrip traces is shown in fig. 3.1.

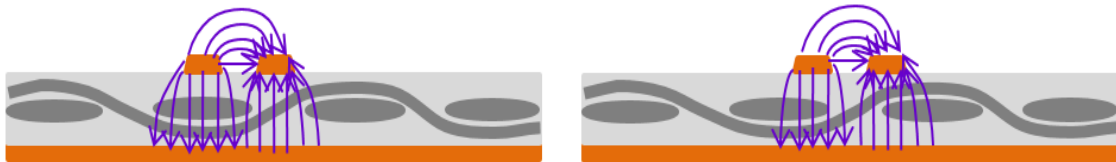


Figure 3.1. Differential Microstrip. Trace 1 is on glass & trace 2 on resin (left), trace 1 & trace 2 are on both glass and resin

In fig. 3.1 (left), trace 1 falls directly above the glass bundle and trace 2 falls on resin. The effective dielectric constant experienced by trace 1 is higher than effective DK experienced by trace 2. EM wave on trace 1 travels at a lesser velocity than on trace 2 which will result in skew. Skew between the differential pair is dependent on the relative location of the traces with respect to the glass bundles. From fig. 3.1 (right), both P & N traces experience similar effective DK since they fall both on glass and resin. Skew between diff. pair in this case can be expected to be lesser than previous case. Due to the

manufacturing tolerances, the PCB fabricator cannot control the location of the trace with respect to glass bundles resulting in trace to trace & board to board variation in skew even though the layout is same. Cross section of a differential stripline traces is shown in fig. 3.2.

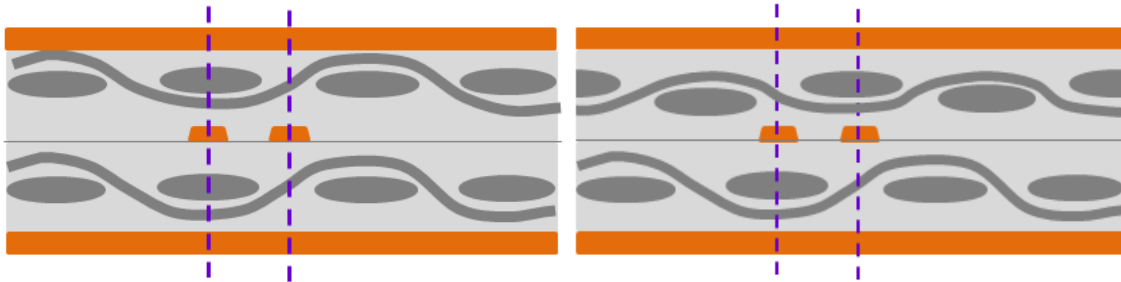


Figure 3.2. Differential Stripline. Bundles are aligned(left), not aligned (right)

In the case of differential stripline, skew is dependent not only on the relative location of traces with respect to glass bundles but also the relative location of glass bundles from dielectric above the trace to the glass bundles in the dielectric below the trace. Worst case skew will be higher when the bundles are aligned as shown in fig.3.2 (left) compared to when bundles are not aligned as in fig.3.2 (right).

3.2. IMPACT OF GLASS WEAVE SKEW

3.2.1. S-Parameters. Due to the difference in wave velocities on different traces, signals arrive at the destination at different times. In a differential pair transmission line as shown in fig. 3.3, a phase difference between the S13 and S24 exists.

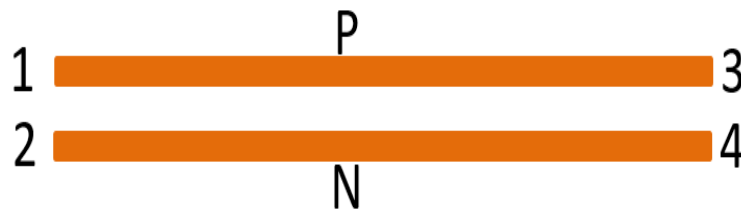


Figure 3.3. Differential pair transmission line

S-parameters can be expressed as either a combination of magnitude and phase or real and imaginary part. When S_{31} & S_{42} are exactly out of phase, they can be expressed as

$$S_{31} = a + j b \quad (3)$$

$$S_{42} = -a - j b \quad (4)$$

Differential insertion loss, S_{dd21} can be calculated from the single ended s-parameters using the equation 3.

$$S_{dd21} = 0.5 * (S_{31} + S_{42} - S_{32} - S_{41}) \quad (5)$$

S_{dd21} can be zero when S_{31} and S_{42} are exactly out of phase. Hence we see a big dip in S_{dd21} [16] when there is a large skew between P & N signals. Single ended measured s-parameters of a test vehicle with high P & N skew is shown in fig. 3.4

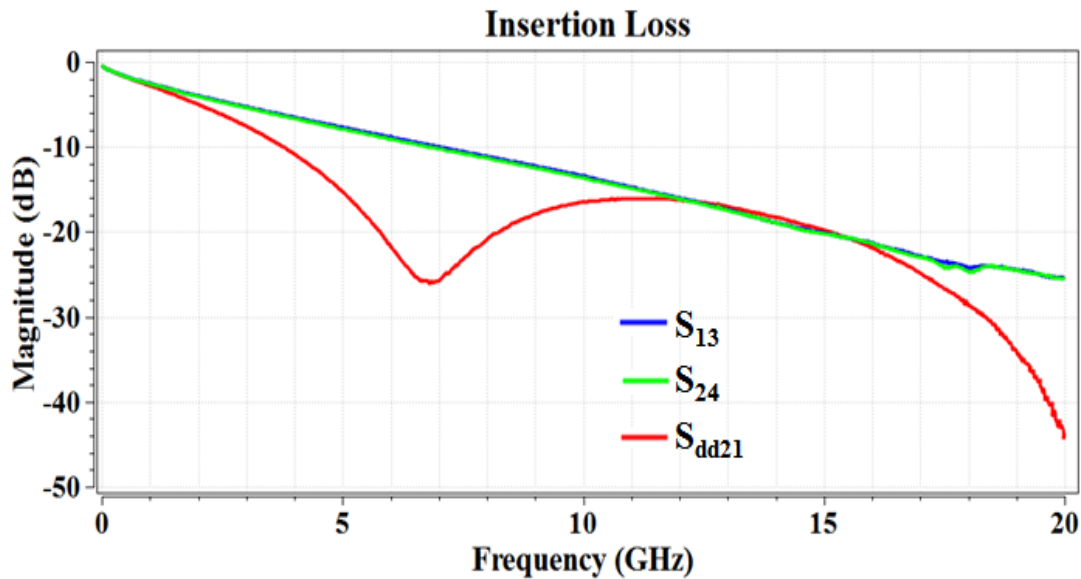


Figure 3.4. Measured single-ended and differential insertion loss of diff. pair with big skew

Phase of S_{13} and S_{24} are plotted in fig. 3.5. It can be observed that the phase difference between S_{13} and S_{24} is nearly 180° in the frequency range 6 – 8 GHz and 17 – 20 GHz, hence there is a big dip in differential insertion loss in those frequency ranges. In the frequency range 12 – 15 GHz, there is small phase difference between S_{13} and S_{24} . As a result, the differential insertion loss is close to single ended insertion. Fig. 3.6 shows the zoomed in phase of S_{13} and S_{24} in the frequency range 3GHz-8GHz.

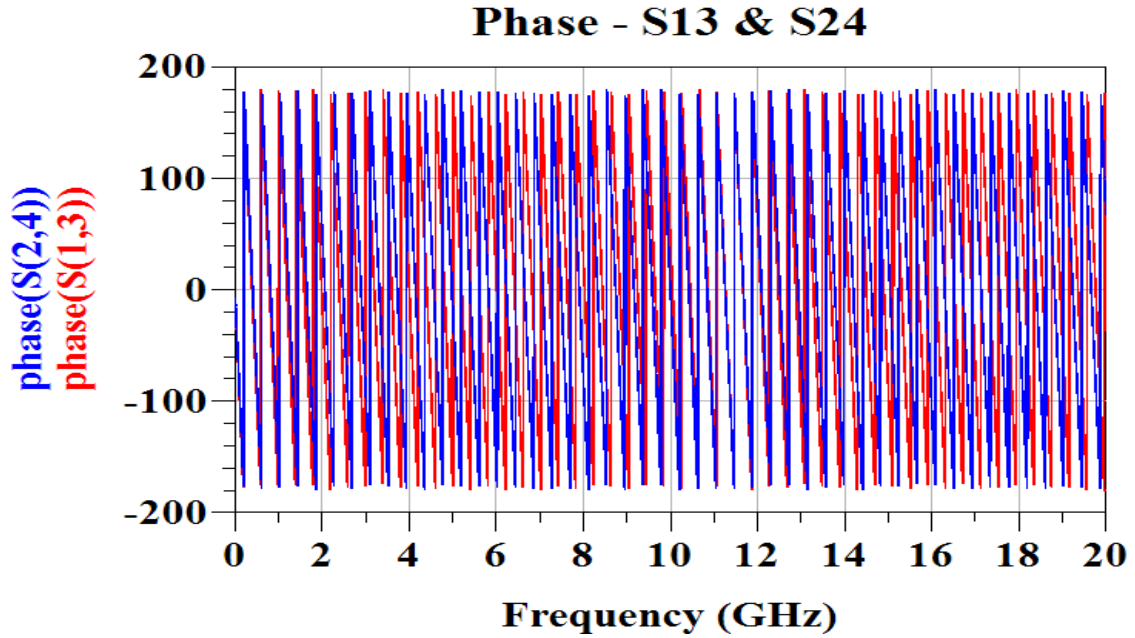


Figure 3.5. Measured single-ended phase – S_{13} & S_{24}

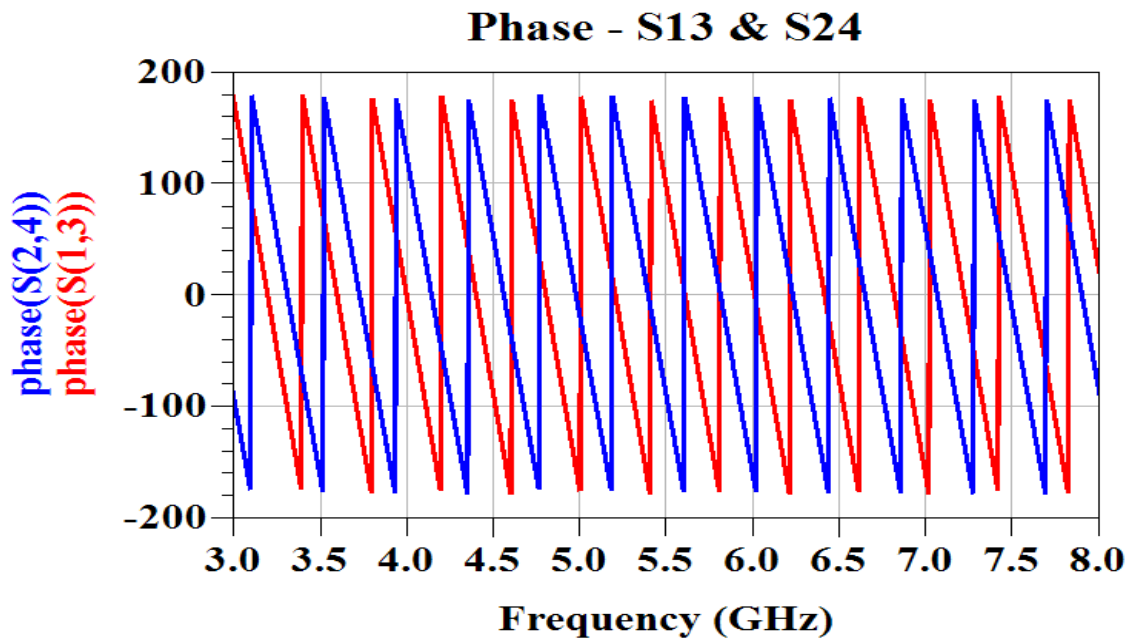


Figure 3.6. Measured single-ended phase – S_{13} & S_{24} (Zoomed in)

3.2.2. Eye Diagram. The eye of differential signal will be degraded significantly since the differential loss is increased because of a big dip. Eye diagram at transmitter and receiver are plotted in fig.3.7.

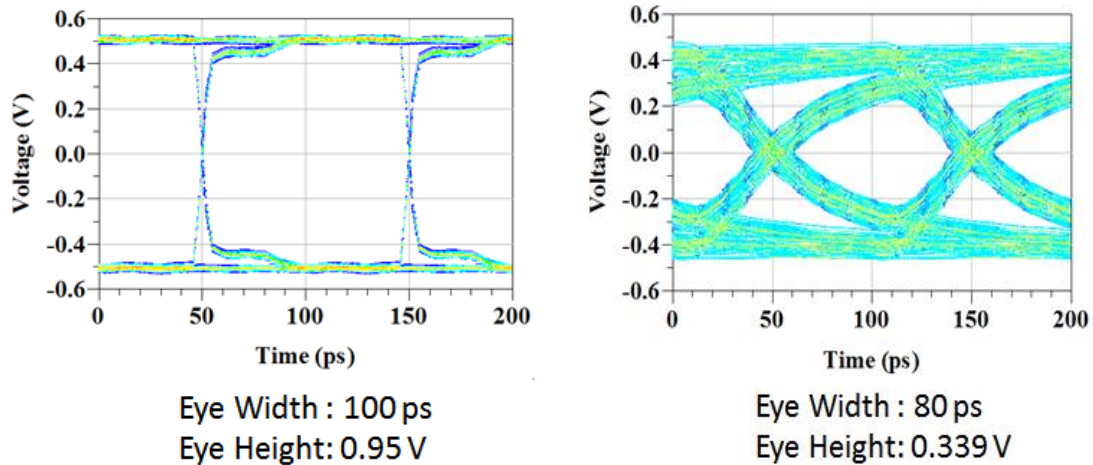


Figure 3.7. Eye of differential signal. At the transmitter (left), at receiver (right)

Fig. 3.7 (left) shows the eye diagram of a differential signal at the transmitter whose data rate is 10 Gbps. After the signal passes through a channel whose loss is 9 dB @ 5GHz, the eye of differential signal at receiver is shown in fig. 3.7 (right). The eye height and eye width is reduced but it is due to the channel loss. Fig. 3.8 shows the eye diagram of differential signal at the receiver after passing through a channel with same loss but with an 80 ps skew contributed by glass weave. Skew between P & N has completely closed the eye. Hence it is very important to reduce the skew.

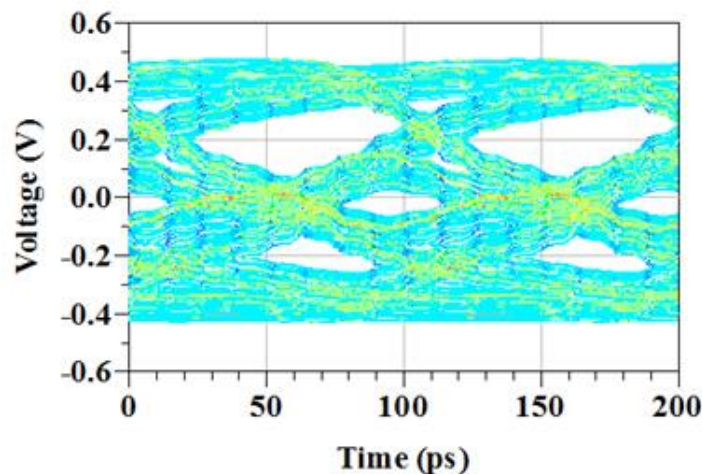


Figure 3.8. Eye of differential signal at the receiver after passing through channel with big skew

4. REVIEW OF SKEW MITIGATION STRATEGIES

Several strategies have been proposed by various studies performed earlier. A review of these strategies and their limitations is presented in this section.

4.1. TRACE ROTATION

Several studies [2], [3], [5], [7], [17], [19], [20] have indicated that the skew between differential pairs can be reduced by rotating the traces. From straight traces shown in fig. 4.1(left) it can be understood that the skew between diff. pair will be considerable since one of the trace is on glass bundle and the other is on resin. By rotating the traces by 10° with respect to glass bundle as shown in fig. 4.1(right), both the P and N traces pass through glass predominant and resin predominant regions thereby partially compensating the difference in velocities of signals travelling on P & N traces.

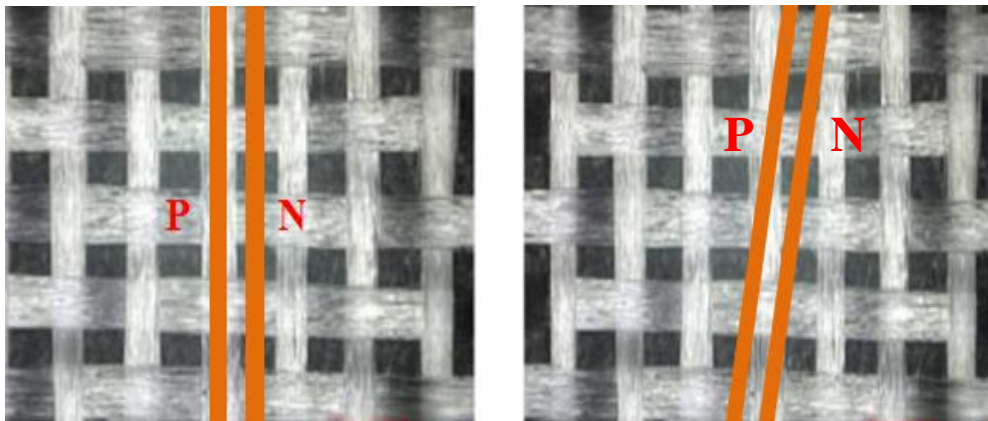


Figure 4.1. Straight trace routing on woven glass (Left), 10° rotated trace (right)

Maximum reduction in skew is claimed to be obtained when the traces are rotated at an angle of about 45° [2]. The difference in percentage of the glass and resin through which the traces traverse will be minimized when the traces are routed at about 45° . Rotating the traces by 45° cannot completely eliminate the skew. In fig. 4.2 (left), P trace passes through resin region (highlighted by yellow rectangular regions) whereas N trace passes through glass region in which case skew will be observed. By visually inspecting

fig. 4.2 (right), it can be observed that both P & N traces goes through identical amount of glass and resin in which case much less skew will be observed .

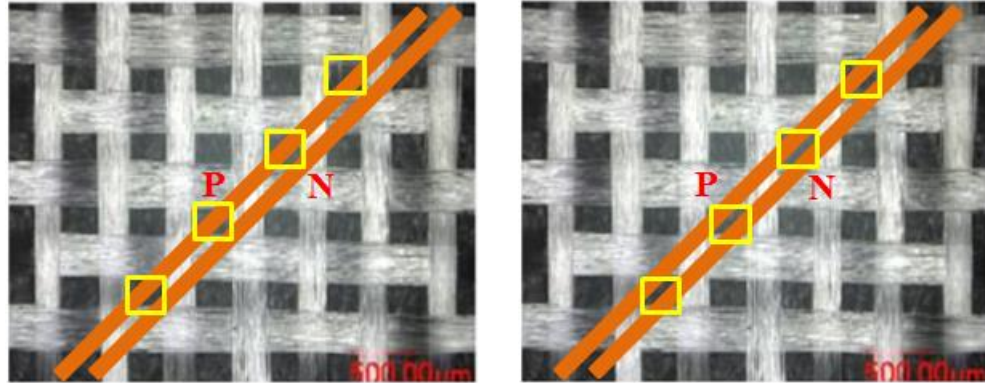


Figure 4.2. Traces rotated by 45°. P is on resin & N is on glass (left), P & N on equal amounts of resin and glass (right)

Limitation of rotating the traces is that it takes more space than straight traces. Since the routing space on the PCB's is limited, board sizes have to be increased so as to accommodate the rotated traces which eventually increases the cost. Another constraint on PCB designs is location of components and ASICs. In few cases it may not be possible to use rotated traces when the ASICs are located at same height on board layout as shown in fig. 4.3. Rotating the traces will also be difficult in back plane applications. This issue can be solved by rotating the panel instead of traces which is explained in the next sub section.

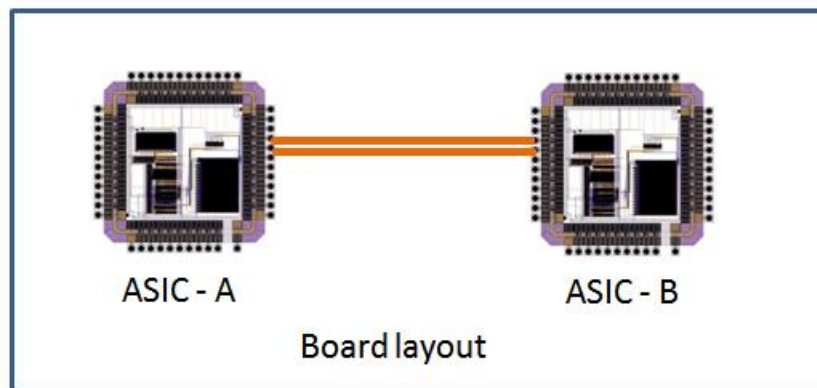


Figure 4.3. ASICs located on same vertical level on board layout

4.2. PANEL ROTATION

In cases where the traces cannot be rotated like in backplane applications, the panel (PCB dielectric) itself can be rotated with respect to the trace as in fig 4.4. A larger PCB panel is needed as the corners of the rotated panel needs to cut off and discarded which will result in more material costs. Rotating the panels will increase the material cost significantly on large PCBs of sizes in the range of 15"-25" long. It is estimated that a mere 10° rotation of the panel will lead to 30% increase in cost to fabricate PCBs of size 18" X 24".

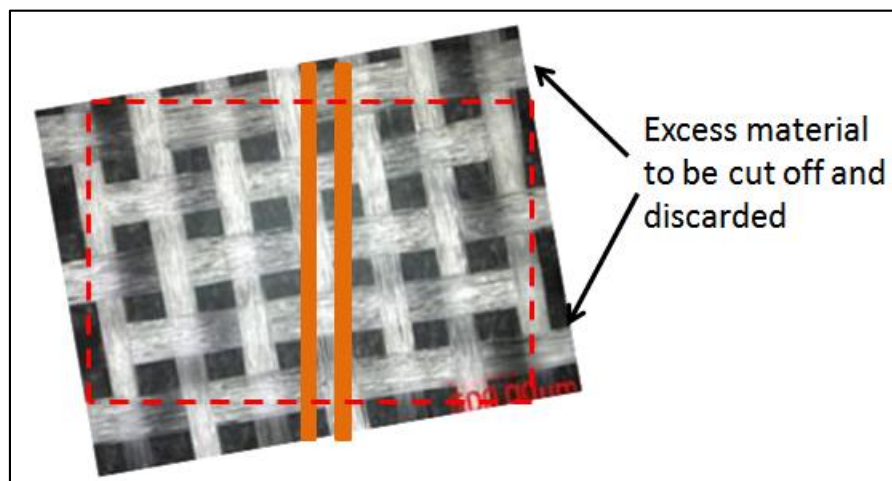


Figure 4.4. Rotated panel with respect to trace

Rotating the laminate panel is an effective strategy for smaller size boards since the material wastage will be less.

4.3. ZIG-ZAG ROUTING

Zig-zag routing can be employed to minimize Skew [9]. This design is a slight modification of rotating the traces at angle with respect to glass bundle. Advantage of this strategy is that it can be used when two ASICs are located at the same height on the board layout as in fig.4.5.

The obvious limitation of this strategy is the routing space. Moreover the length of the traces/links will be more when compared to straight traces thereby increasing the loss of the channel. As it is widely known that the eye of the signal degrades with

increase in data rates and with increase in loss at the Nyquist frequency, it is important to consider if the BER is in acceptable range with this increase in loss due to increased length of the channel by zig-zag routing. There is an additional degradation in the eye due to multiple discontinuities.

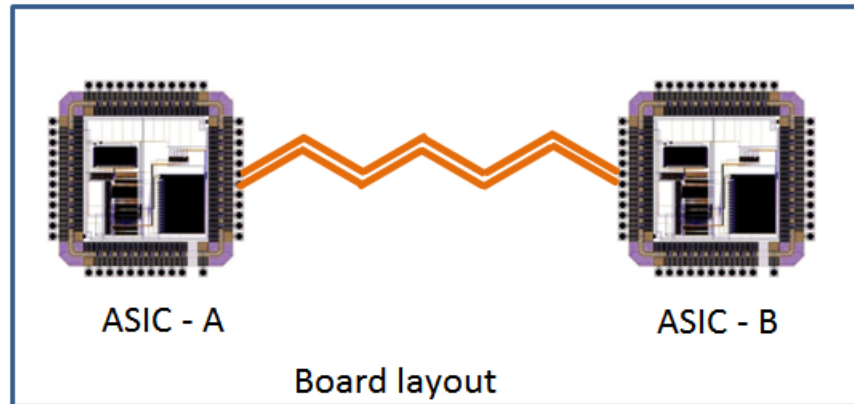


Figure 4.5. Zig-Zag routing between two ASICs

4.4. USING SPREAD GLASS

The local variations in the dielectric constants in the substrate can be reduced by reducing the gaps in the glass weave bundle which are filled with the epoxy material (resin) when the laminates are fabricated. Thickness of the glass bundles can also be reduced so as to reduce the effective DK difference between trace falling on glass bundle and the trace that falls on resin region. Square glass fabric is obtained after weaving which is spread by spreading companies (may be same as glass company). Spreading process reduces the thickness of glass and reduces the gaps between glass bundles. Cross-section and top view of 1037 square and spread glass are shown in fig. 4.6 & fig 4.7.

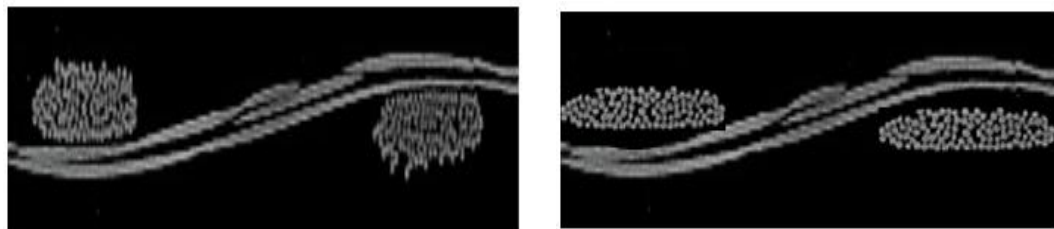


Figure 4.6. Cross-Section view of 1037 glass. Square glass (left), spread glass (right)

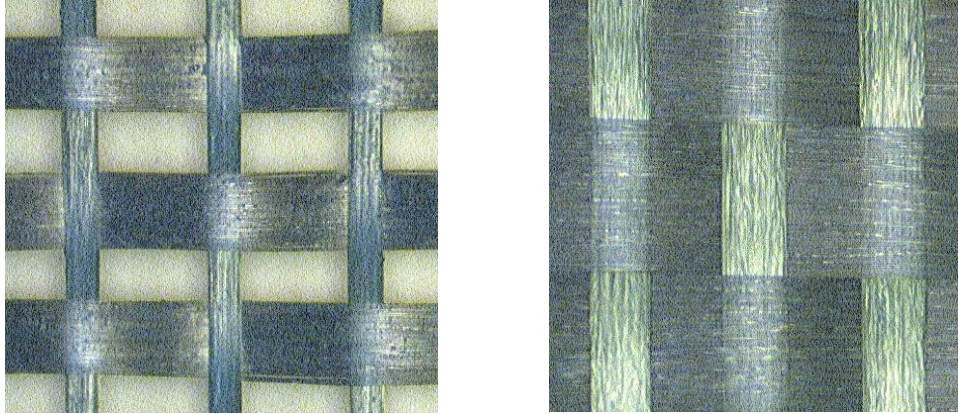


Figure 4.7. Top view of 1037 glass. Square glass (left), spread glass (right)

Spread glass is being more widely adopted in the industry as it is shown to reduce skew at a mere 5% increase in cost. Super spread glass with ultra-thin glass bundles are also available but at a premium price. For low volume, high cost products like routers and servers it is common to use super spread glass. But for high volume products which are cost sensitive, it is not feasible to use super spread glass. This study will focus on the performance in terms of skew of spread glass and not on super spread glass.

4.5. USING LOW DK GLASS

Low DK glass has a lower dielectric constant (~ 4.5) compared to the standard glass (DK ~ 6). Reducing DK difference between glass and resin by using low DK glass is suggested to be one of the ways to reduce the skew [5], [9]. The dielectric constants of different materials are tabulated in table 4.1.

Table 4.1. Dielectric constants of glass and resin

Material	Dielectric constant (dk)
Standard Glass	~ 6
Low DK Glass	~ 4.5
Resin	~ 3.5
Ultra-Low DK glass	~ 3.5

Several studies [2], [5], [11] reported that the worst case skew when straight traces are routed on E-glass can be as high as 15ps/inch. Moving to low DK glass increases cost of PCB by 25% but has an added advantage of lower dielectric loss. In this study, the performance of low DK glass in terms of skew is measured on the designed test vehicles. Low DK glass is evaluated to see if this strategy can be employed to offer a cost effective solution to reducing skew on 15"-20" long traces in this work. Although low DK glass has lower DK compared to standard glass, there is still a difference between DK's of glass and resin. Few of the glass manufacturers offer ultra-low DK (~3.5) glass but at much higher cost.

4.6. USING MULTI-PLY DIELECTRICS

Intra-pair skew can be mitigated by using the averaging effect when multiple ply's of glass fabrics are used when a dielectric is made. Stripline routed on single ply and dual ply fabric are shown in fig.4.8 (left) & fig. 4.8 (right).

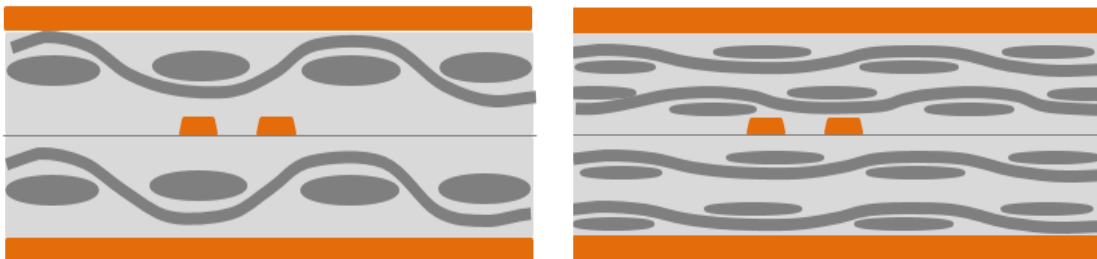


Figure 4.8. Stripline on 1-ply glass dielectric (left), 2-ply glass dielectric (right)

Gaps in one ply may be covered partially/fully by the glass bundles of second ply as shown in fig 4.8 (right) thereby reducing the inhomogeneity. It can be observed that the glass fabric needs to be thinner for dual ply when compared to single ply to make a dielectric of particular thickness. The worst case skew occurs when all the four glass bundles line up in dual ply dielectric case which is highly unlikely.

5. MEASUREMENT OF GLASS WEAVE SKEW

5.1. DESIGN OF TEST VEHICLES

Test vehicles are designed to experimentally measure the skew on 1-ply spread glass, 2-ply spread glass, in fill and warp directions, standard glass and low DK glass. Six different test vehicles with three different trace pitches namely Pitch 'A', Pitch 'B', Pitch 'C' are fabricated whose stack up is specified in fig. 5.1.

			Thickness	Dk (2GHz)	Df(2GHz)
Top			2.2		
	1-ply	Glass-X	4.8	3.7	0.006
G02			0.6		
	2-ply	Glass-X	5	3.63	0.007
T03			0.6		
	2-ply	Glass-X	5	3.5	0.007
G04			0.6		
	2-ply	Glass-Y	6	3.17	0.007
T05			0.6		
	2-ply	Glass-Y	5.8	3.14	0.006
G06			0.6		
	1-ply	Glass-X	5	3.72	0.006
T07			0.6		
	1-ply	Glass-X	5.1	3.6	0.007
G08			0.6		
	1-ply	Glass-Y	5	3.26	0.006
T09			0.6		
	1-ply	Glass-Y	4.6	3.24	0.006
G10			0.6		
	1-ply	Glass-X	5	3.63	0.007
G11			0.6		
	1-ply	Glass-Y	4.6	3.24	0.006
T12			0.6		
	1-ply	Glass-Y	5	3.26	0.006
G13			0.6		
	1-ply	Glass-X	5.1	3.6	0.007
T14			0.6		
	1-ply	Glass-X	5	3.6	0.006
G15			0.6		
	2-ply	Glass-Y	5.8	3.14	0.006
T16			0.6		
	2-ply	Glass-Y	6	3.17	0.007
G17			0.6		
	2-ply	Glass-X	5	3.5	0.007
T18			0.6		
	2-ply	Glass-X	5	3.63	0.007
G19			0.6		
	1-ply	Glass-X	4.8	3.7	0.006
Bottom			2.2		


 BackDrill

Figure 5.1. Stack up of test vehicles

Each test vehicle is a 20-layer board with microstrip differential traces on top and bottom layers, stripline differential traces in inner layers. The microstrip traces are routed on only 1-ply spread glass whereas stripline differential pairs are routed on 1 ply as well as 2 ply spread glass. All the traces are straight traces (not rotated) routed in west-east direction on layers top, T03, T05, T07, T09 and in the north-south direction on layers T12, T14, T16, T18, bottom. The stack up is symmetrical about layer 10, 11. For example, T03, T18 are in 2-ply spread glass-X; T05, T16 are in 2-ply spread glass-Y; T07, T14 are in 1-ply spread glass-X; T09, T12 are in 1-ply spread glass-Y.

Glass dimensions like glass bundle thickness, bundle width and gaps in the glass fabric vary with the glass style. These details are not specified in standards like IPC but, can be obtained from the glass manufacturer or laminate manufacturer. Table 5.1 shows the glass widths of 1-ply and 2-ply spread glass in warp and fill directions. It can be observed that the glass dimensions are different in warp and fill direction. The degree of spreading also contributes to the difference in glass dimensions in warp and fill direction. As the warp yarn are held tight, spreading is not very effective on warp when compared to fill direction.

Table 5.1. Glass bundle widths in fill and warp directions (from laminate fabricator)

Glass Style	Warp Width (mils)	Fill Width (mils)
1-ply spread glass	14	16
2-ply spread glass	11	17

The thickness of each layer, dielectric constants, and loss tangents of each laminate is specified in the fig. 5.1. Dielectric fabricator usually specifies the effective DK, DF of the laminate from the DK of glass and resin as described in eq.1. On pitch 'A' test vehicles, the center to center distance of the traces in all layers is 'A' mils and the linewidths of the differential pairs are adjusted to give 100 ohm differential impedance on the specified stack up. The center to center distance between the traces is fixed to B mils

on pitch ‘B’ test vehicle and the trace widths are adjusted to give 100 ohm differential impedance similar to other boards.

5.1.1. Footprint Via Optimization. Top launch connectors like 2.4mm, 3.5 mm, 2.92 mm, etc. take much more space than microprobes. Moreover, significant cost of connectors is involved since each differential pair needs 4 connectors. To address the problem of space constraints and connector costs, 1000um GSSG microprobe footprints are chosen for test vehicles. Differential traces routed along the west-east direction on layers Top, T03, T05, T07, and T09 can be seen on board layout as in fig. 5.2.

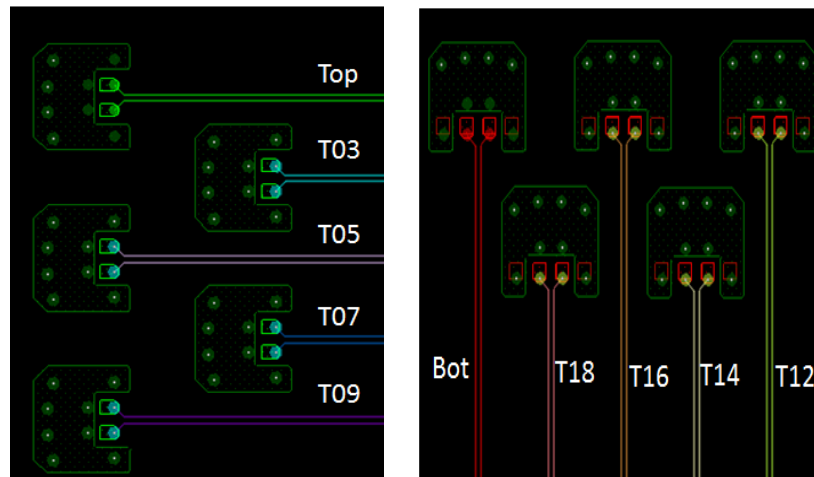


Figure 5.2. Footprints on test vehicles. West-East direction (left), North-South direction (right)

It is important to design the launch carefully in order to minimize the reflections and ensure the maximum transmission of energy into the transmission line. The fields near the probe launch are non-TEM mode due to the presence of discontinuities like vias. Hence full wave simulations for the probe footprint alone are performed in HFSS so as to minimize the return loss. The target return loss is -20 dB over a frequency range 10 MHz – 20 GHz. When the return loss cannot be brought below -20 dB below 20 GHz, the target is relaxed to -20 dB up to 15 GHz and below -15 dB between 15 GHz and 20 GHz. Fig. 5.3 shows the HFSS models of microstrip and stripline (T03) probe launches. Additional space of 50 mil is added in both +Z and -Z directions so as not to disturb the fields. All the boundaries are defined as radiation boundary. Discrete ports are used

between the probe landing pads and ground to excite the differential pair. A wave port is defined on the trace side. Adaptive meshing is performed at 20 GHz and the maximum δ between consecutive passes for adaptive solution is specified as 0.02.

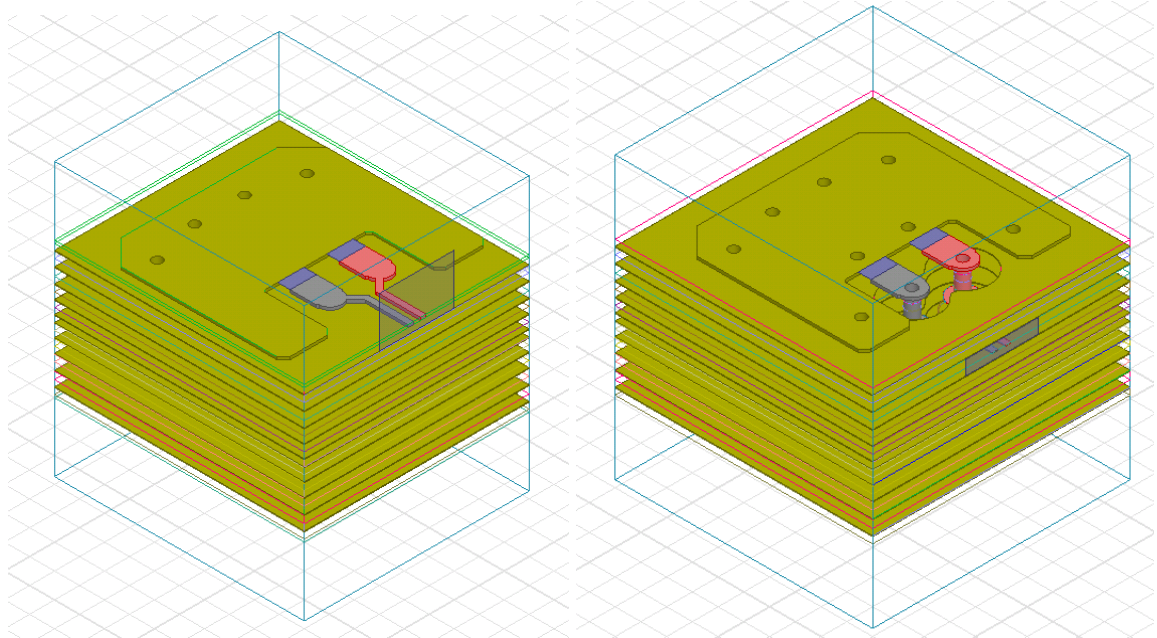


Figure 5.3. HFSS model of probe launch for microstrip (left), Stripline (right)

The signal vias of striplines T03, T05, T07, and T09 are back drilled from the bottom leaving a 7 mil long via stub. Back drilled vias for T03 is shown in fig. 5.4.

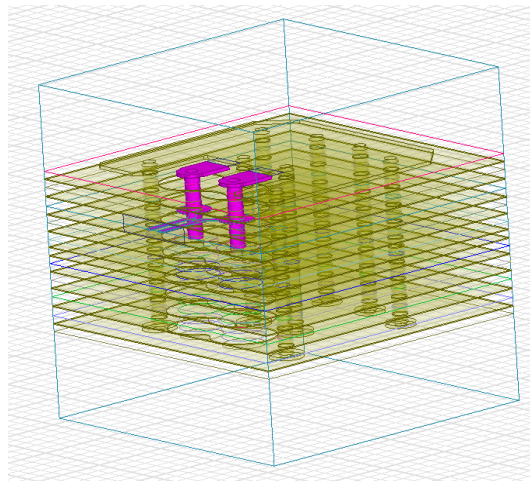


Figure 5.4. Back drilled signal vias in probe launch for stripline T03

Optimized probing pad footprints are used on layout and controlled impedance differential traces are routed. Simulated return loss of the probe launch for microstrip (Top), T03, T05, T07, T09 are shown in fig. 5.5 – fig. 5.9.

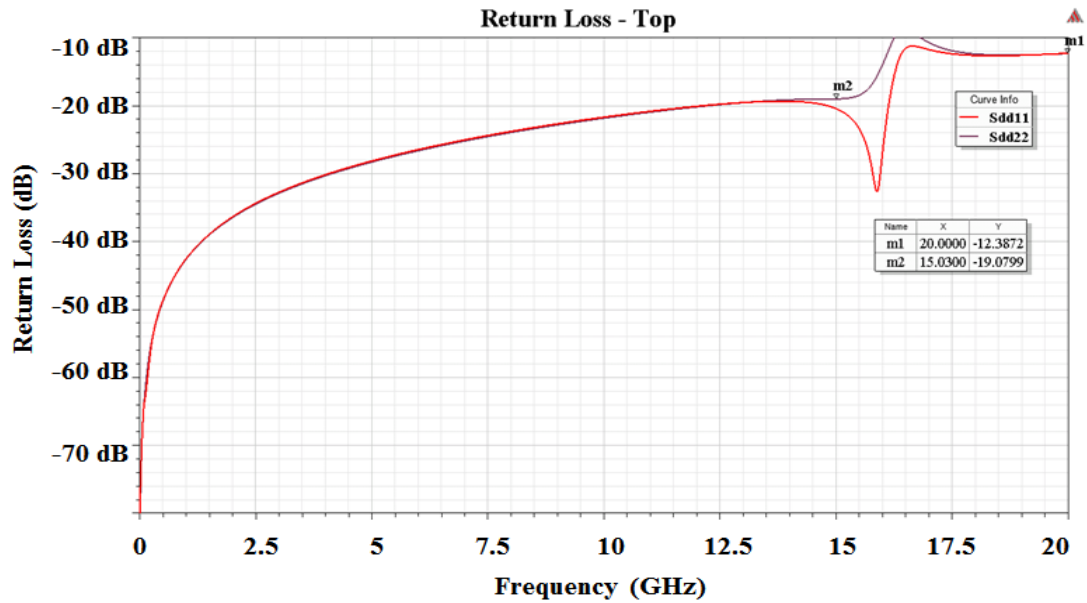


Figure 5.5. Return Loss – Probe launch for Top layer

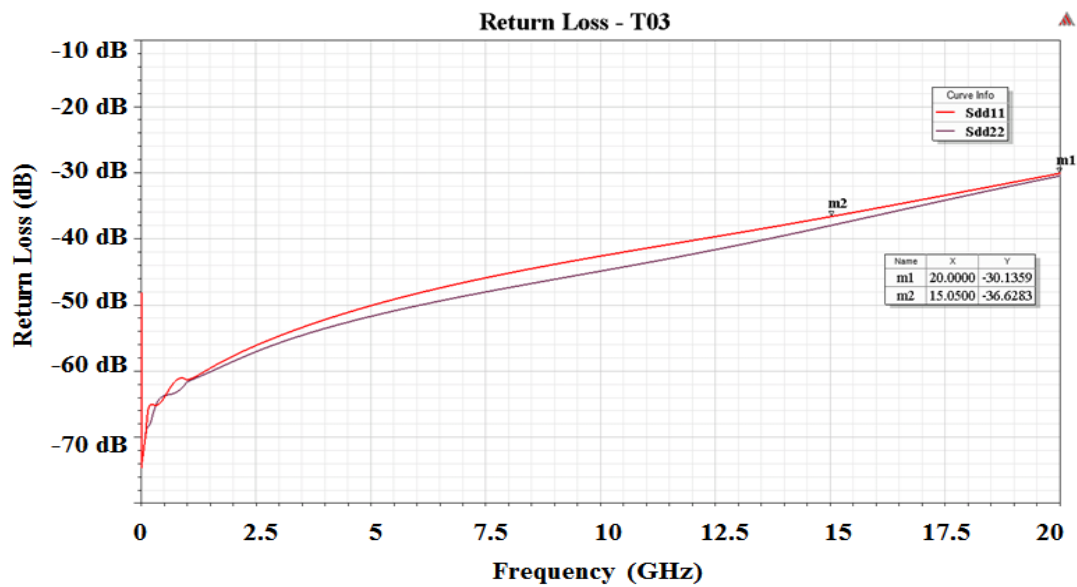


Figure 5.6. Return Loss – Probe launch for T03 stripline layer

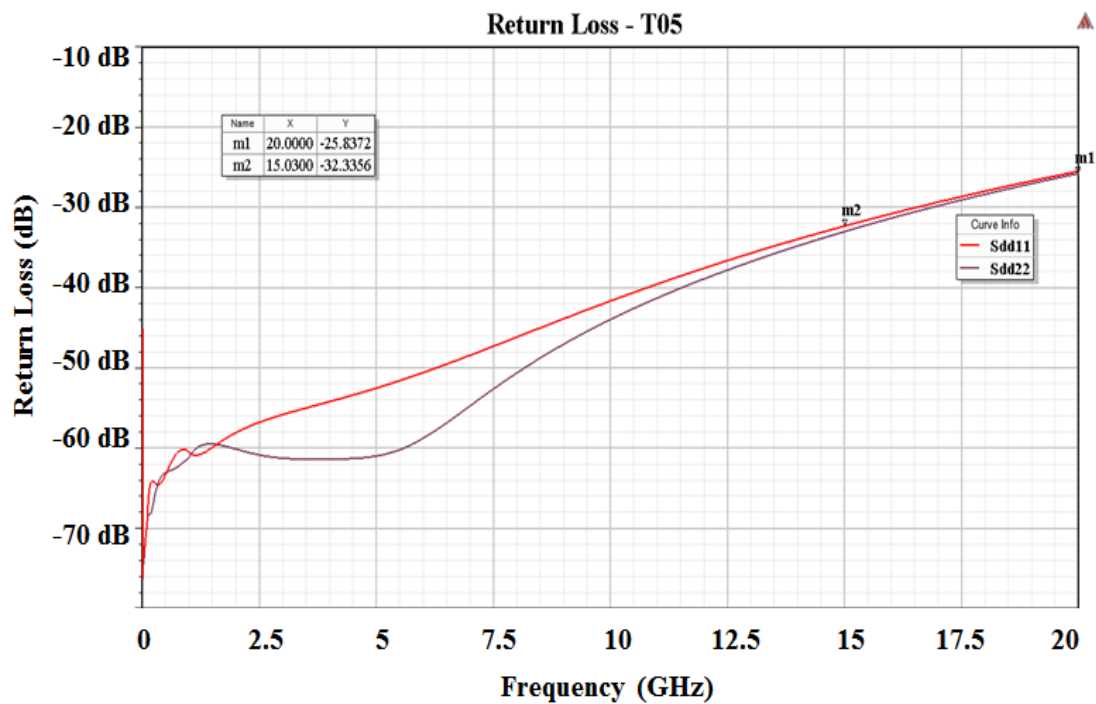


Figure 5.7. Return Loss – Probe launch for T05 stripline layer

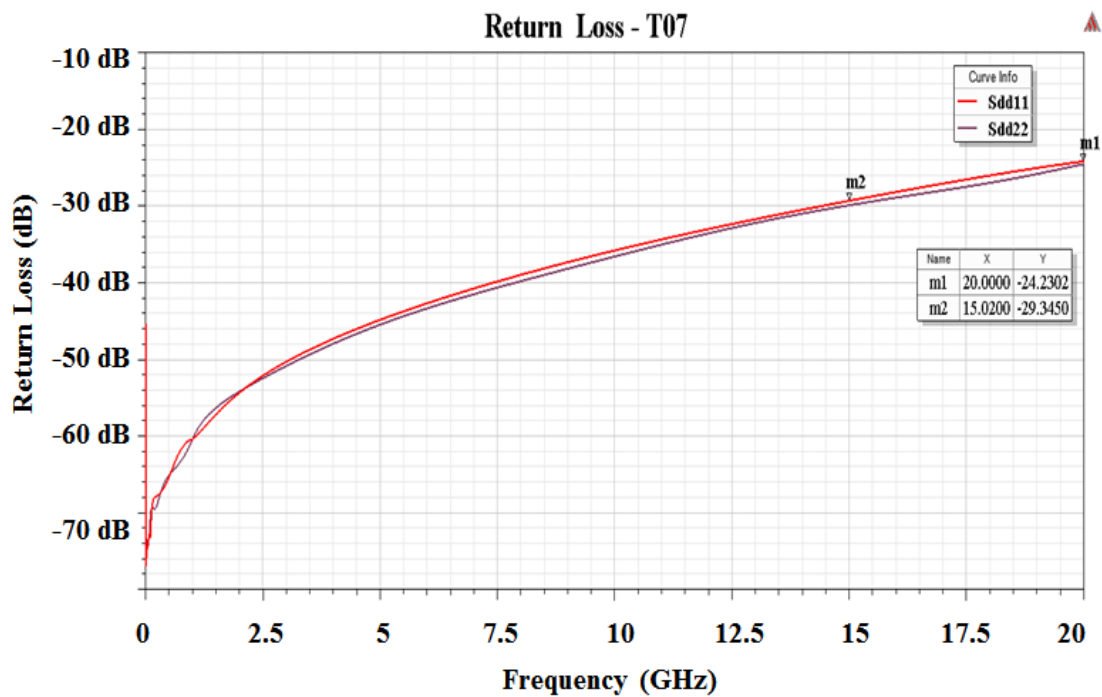


Figure 5.8. Return Loss – Probe launch for T07 stripline layer

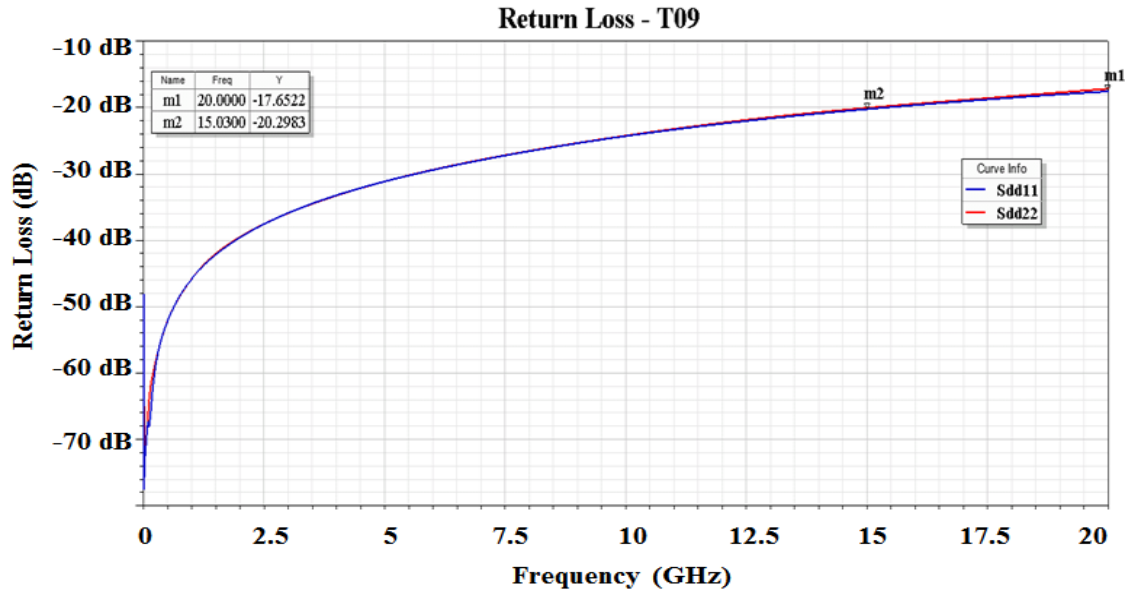


Figure 5.9. Return Loss – Probe launch for T09 stripline layer

5.1.2. Routing Strategy. Differential pairs routed on glass weave are shown in fig. 5.10. During the PCB fabrication, the location of the trace with reference to the glass bundle is statistical and it cannot be controlled. Several studies which were done in the past placed the traces on the board randomly. When done so, the probability of hitting the worst case skew is left to chance.

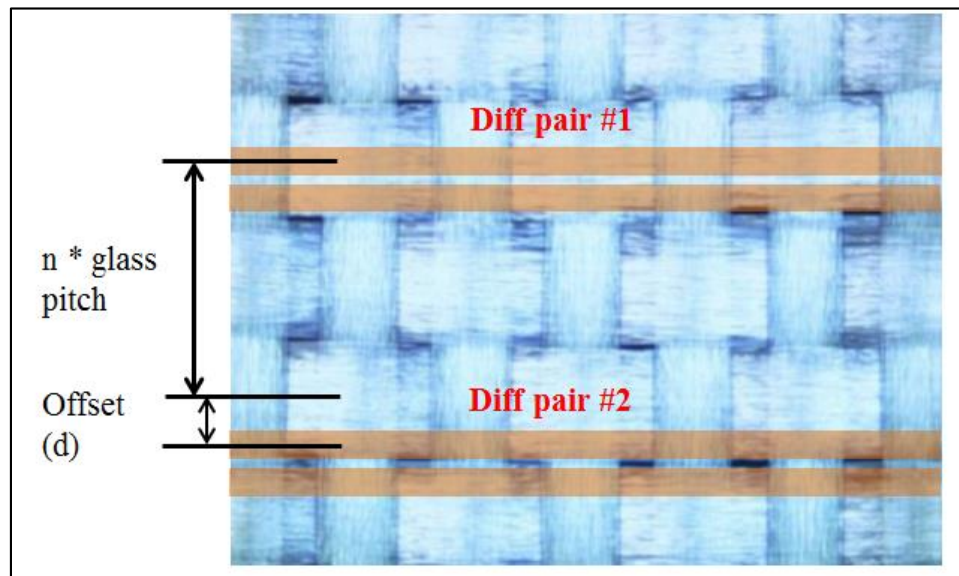


Figure 5.10. Differential pair routing strategy

To increase the probability of hitting worst case skew, the traces are routed in such a way that relative distance of trace to the bundle is increased by an offset (d) of 2 mils for every differential pair as shown in fig. 5.10.

Each of the test vehicles has 180 traces which are 15 inch long in various layers. Fig. 5.11 shows the top side of the test vehicle.

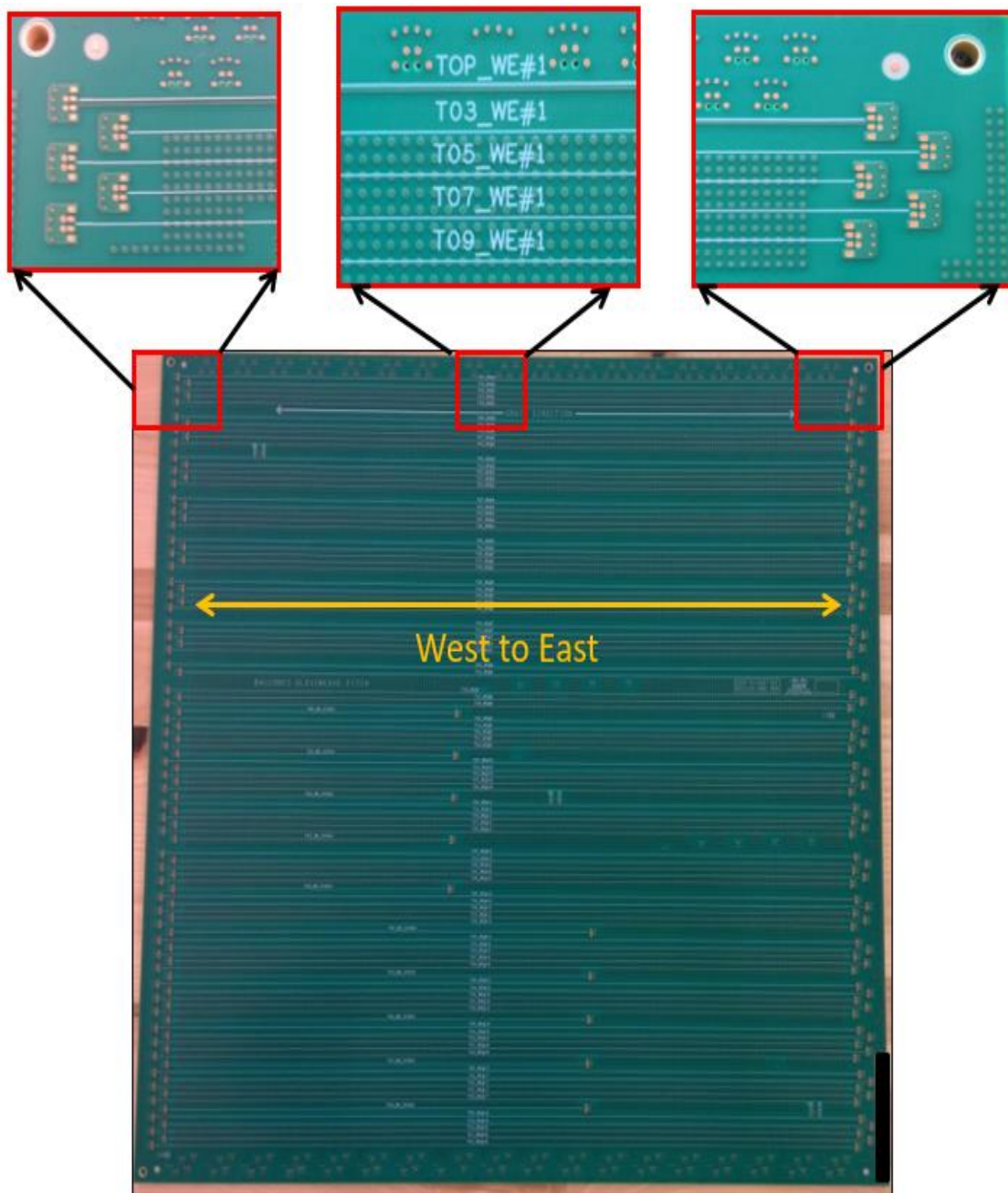


Figure 5.11. Top side of test vehicle

Footprints of 1000um GSSG probes can be seen on top side of the board. Differential pairs are routed in west-east direction on layers Top, T03, T05, T07, and T09 which can be seen from the silk screen on top layer. The excess via stubs on T03, T05, T07 and T09 are back drilled from bottom. Bottom side of the test vehicle is shown in fig 5.12.

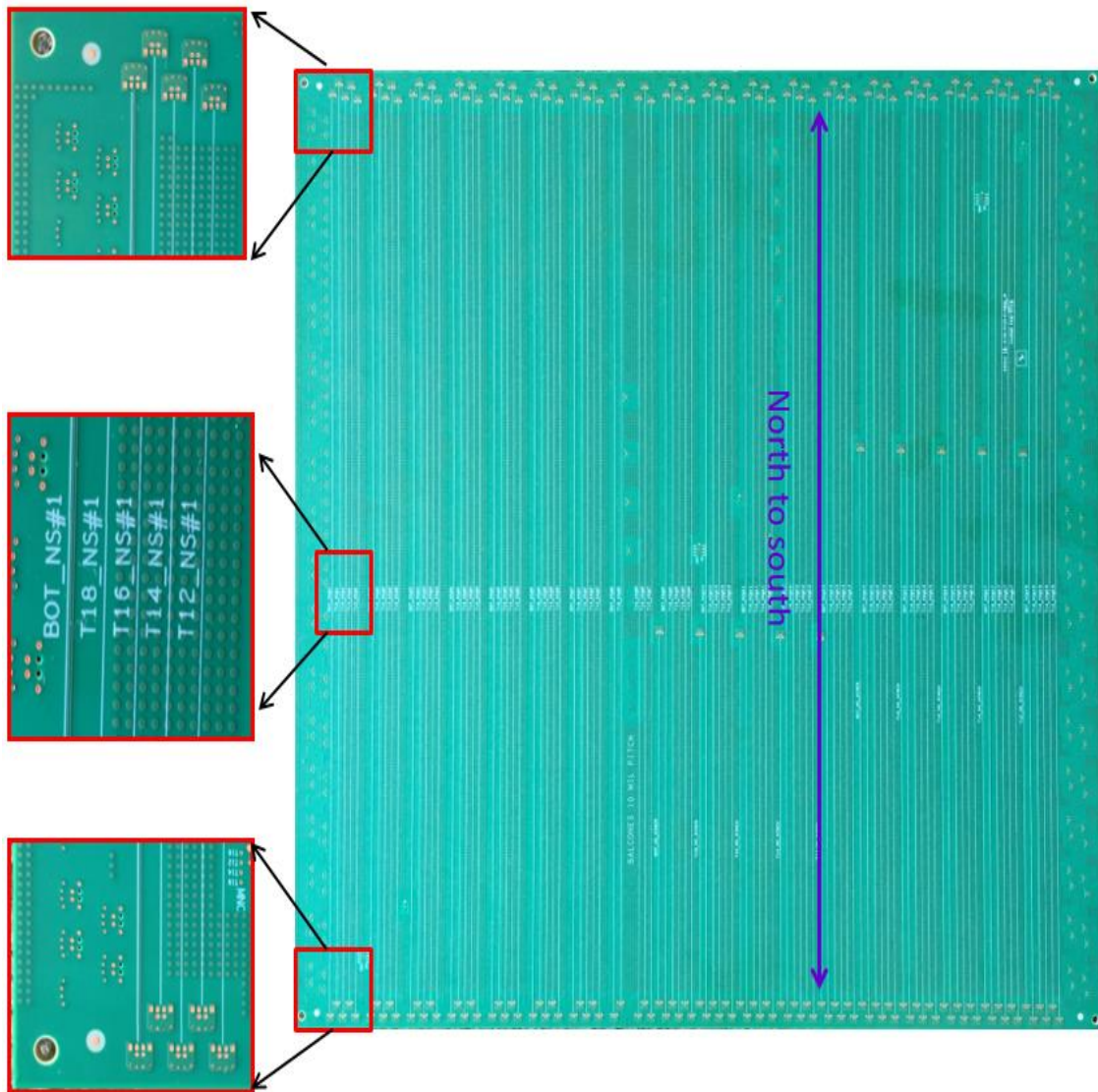


Figure 5.12. Bottom side of test vehicle

All the differential pairs in layers T12, T14, T16, T18 and bottom are routed in north to south direction which can be seen on the silk screen on bottom layer. The via

stubs are back drilled from top on layers T12, T14, T16, T18, Bottom. The probe footprints for these differential pairs can be seen on bottom layer in fig. 5.12.

5.2. MEASUREMENT SETUP

GTL4060 probing station from GigaTest labs is used to position the microprobes and the test vehicle. Agilent PNA E8363B (10MHz - 40GHz) is used to measure the s-parameters of the differential traces. Low loss PNA grade cables are used to connect the microprobes to the PNA as shown in the fig. 5.13. Care has to be taken to make sure that PNA cables do not exert pressure on the probes. The probes are extremely sensitive and can break very easily. The probes are mounted on the probe positioners tightly and the test vehicle is held stable using the PCB fixture kit. A suction pump is used to make the PCB fixture kit stationary. The probe can be moved in X, Y, Z directions using the knobs on the probe positioners. The microprobes can be landed on the probing pads carefully using the knobs on the probe positioners by looking into the microscope. Close up picture of probe landing on the test vehicles is shown in fig. 5.14 (left), picture when viewed from microscope is shown in fig. 5.14 (right).

Ground flaps are usually 50um lower in height than the signal pins. The probe can be tilted using a knob on the probe positioner in order to make the tips of signal pins in same vertical level and tips of ground flaps in same vertical level. The ground flaps touch the ground pads when moving the probe downwards before the signal pins touch signal pads. The probes have to be moved about 2-3 mils downwards after the signal pin makes a contact with the pads in order to get a good electrical contact.

Frequency range of the measurement is 10 MHz- 20GHz. It has been observed that 1000um GSSG probes are good only up to 15 GHz. Hence while post processing only data till 15 GHz is used. In order to measure up to a higher frequency range, footprints have to be changed to 750 um GSSG, 500um GSSG or 1000um GSG-GSG probes. Power level is set to -5 dBm, IF bandwidth is set to 5 KHz to reduce the measurement time. Effect of PNA cables and the microprobes are calibrated out using SOLT calibration to move the reference plane to the end of the probes. Calibration is performed using CS3-1000 calibration substrate from GGB industries as shown in fig. 5.15.

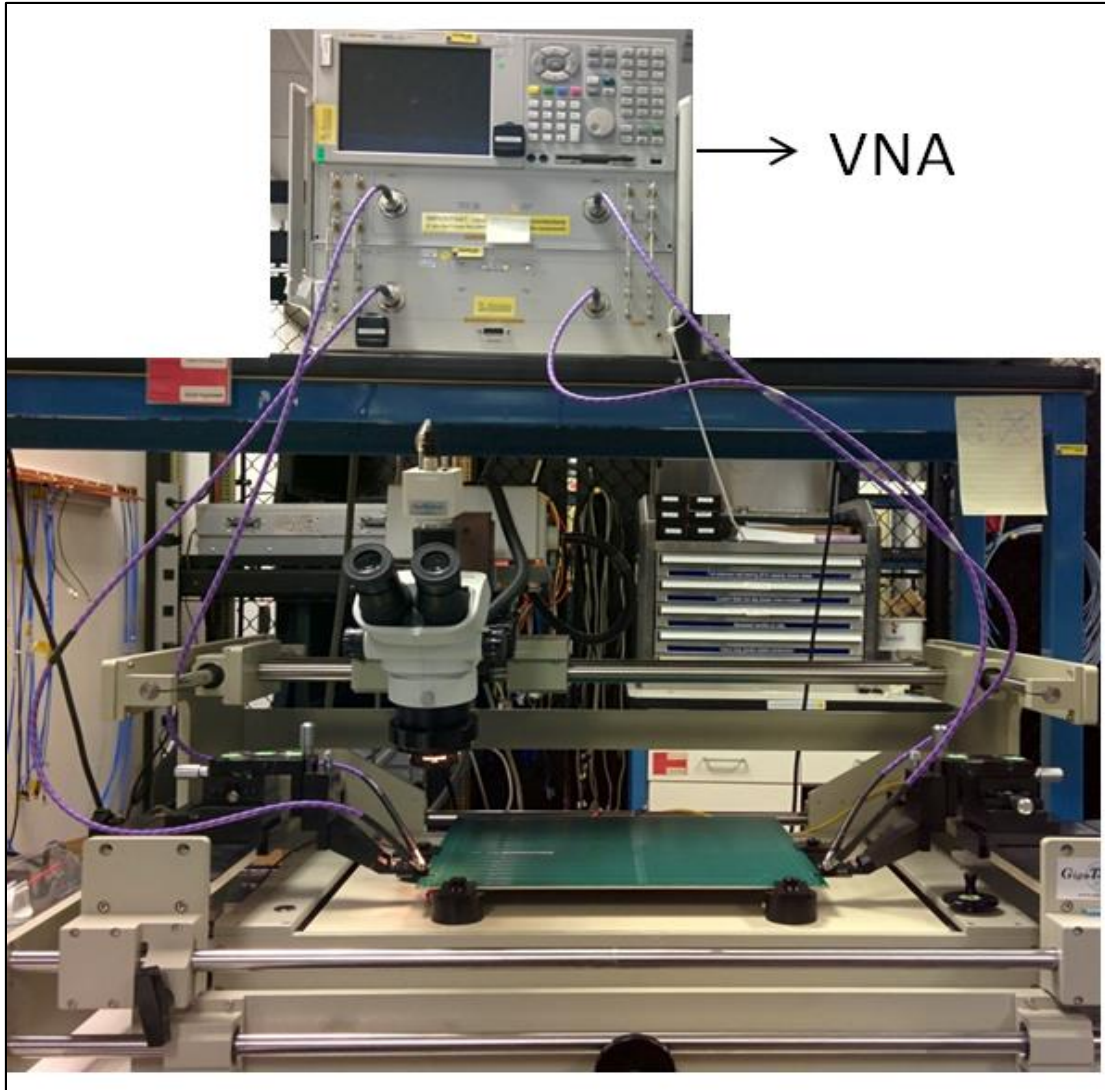


Figure 5.13. Measurement setup – PNA and Microprobe station

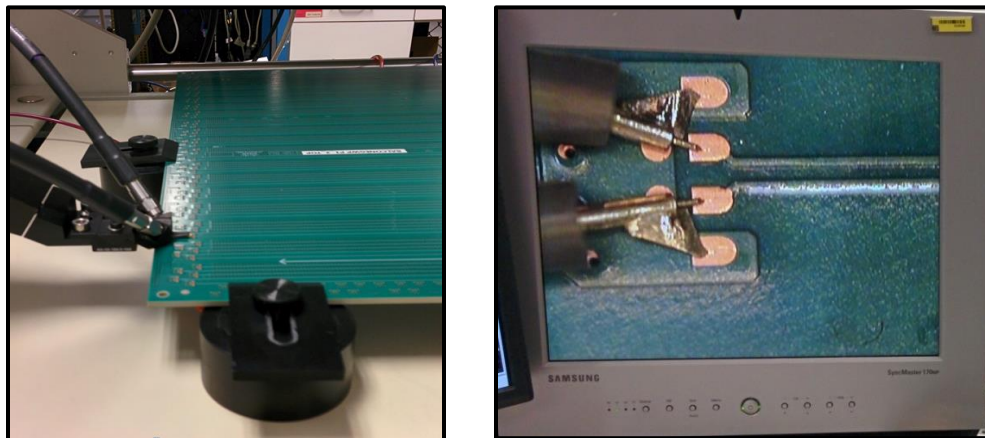


Figure 5.14. Probe landing on DUT. Close up view (left), from microscope (right)

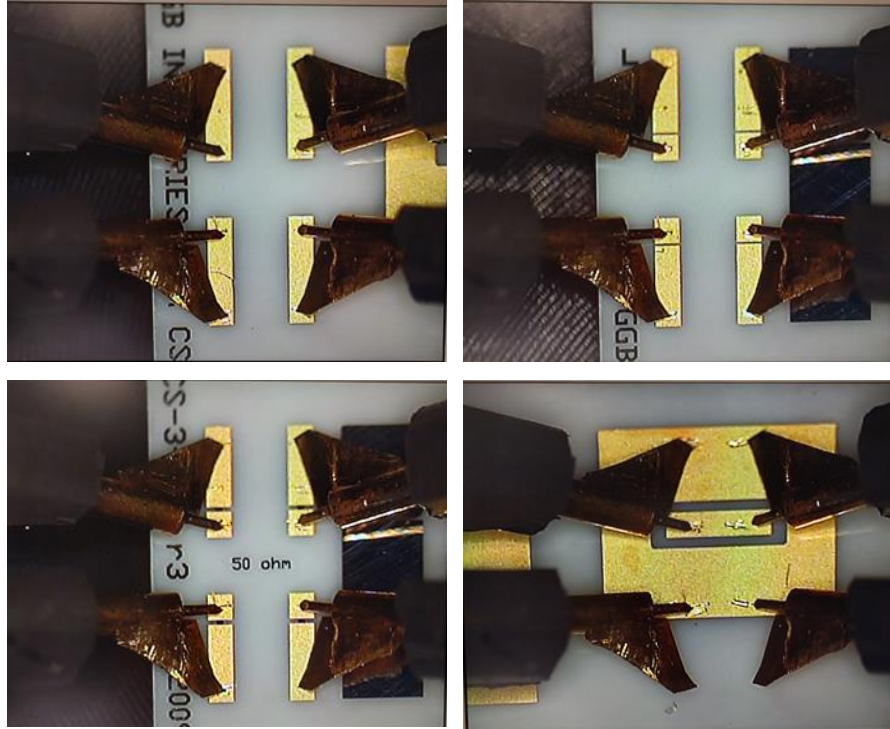


Figure 5.15. Probe calibration on CS3-1000 substrate. Short (top left), Open (top right), load (bottom left), thru (bottom right)

Transient solution in ADS software from Keysight technologies is used to calculate TDT from the measured s-parameters. ADS circuit is shown in fig 5.16.

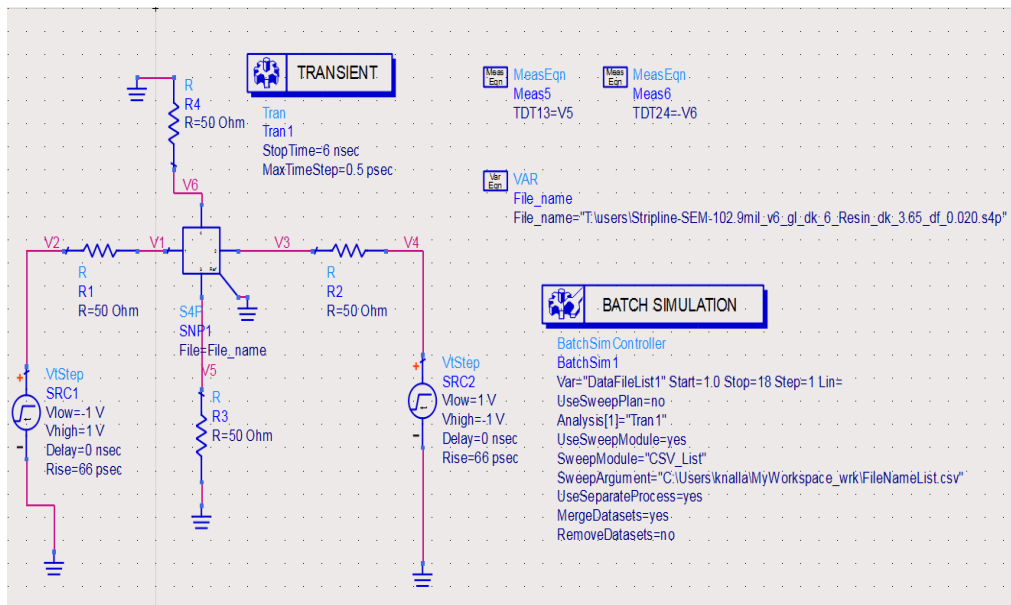


Figure 5.16. ADS Circuit for TDT from S-Parameters

TDT13 is the voltage seen at port 3 when a step excitation is given at port 1 whereas TDT24 is the voltage seen at port 4 when a step signal is given at port 2. TDT13, TDT24 is plotted in fig 5.17. Skew is defined as the difference in zero crossing times of TDT13 and TDT24.

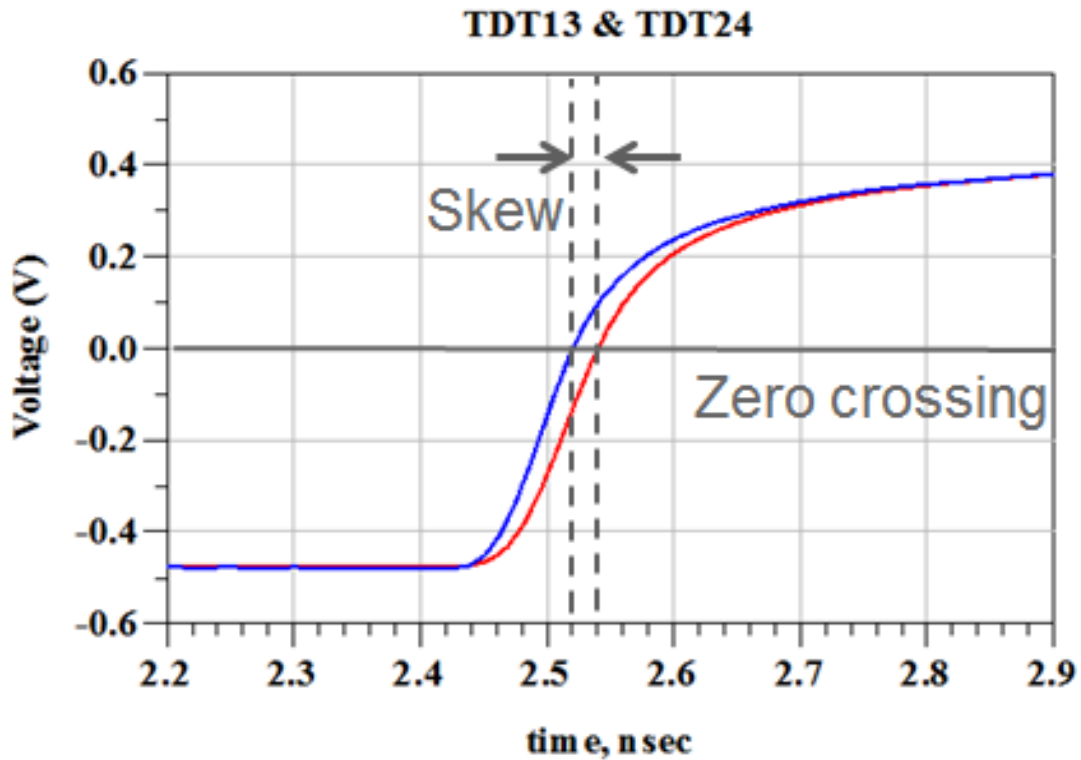


Figure 5.17. TDT from S-Parameters

5.3. RESULTS AND DISCUSSION

S-parameter measurements are taken on differential microstrip and stripline traces on pitch 'A', 'B', 'C' routed on glass X, Y in North-South, West-East directions. Skew per inch is obtained by dividing the skew calculated from TDT by 15 since the traces are 15 inch long. The comparison of skew per inch between pitch 'A', 'B', 'C' routing in North-South, West-East directions is presented in this section. A comparison of skew on stripline between glass X, Y on 1-ply and 2-ply spread glass is also presented. Two boards with differential trace pitch 'A', one board with pitch 'B' and three boards with pitch 'C' were fabricated. Boards can be identified by the names B1, B2, B3 in the below plots.

5.3.1. Microstrip – Pitch A, B, C. Comparison of pitch A, B, C differential routing in terms of skew per inch on microstrip traces in West-East, North-South directions are plotted in fig. 5.18 & 5.19. It can be observed from below plots that the skew per inch is considerably different on different routing directions.

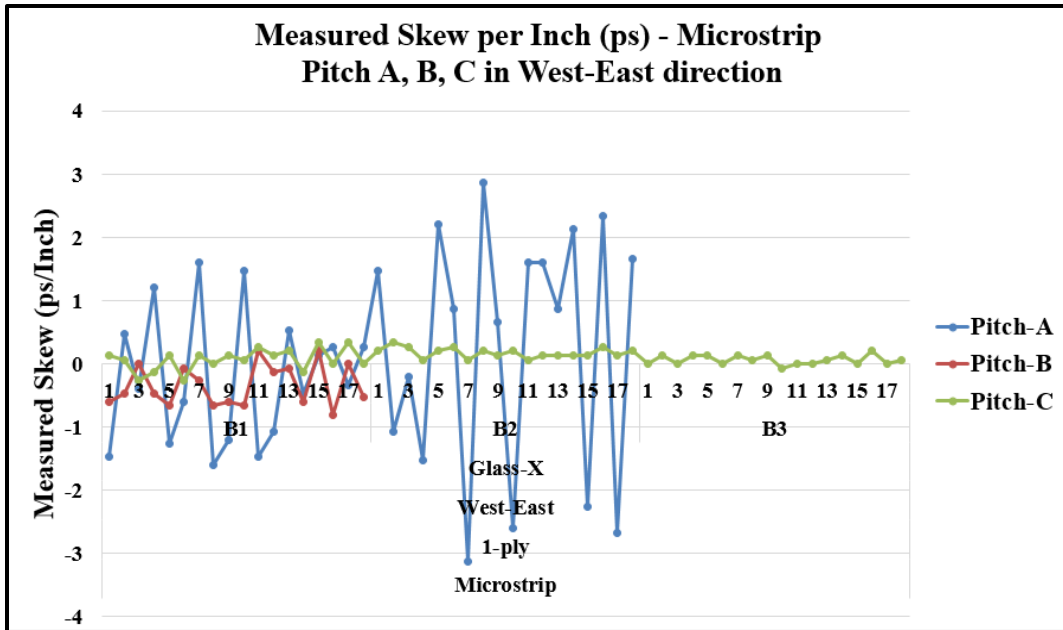


Figure 5.18. Skew on microstrip in West-East routing – Pitch A, B, C

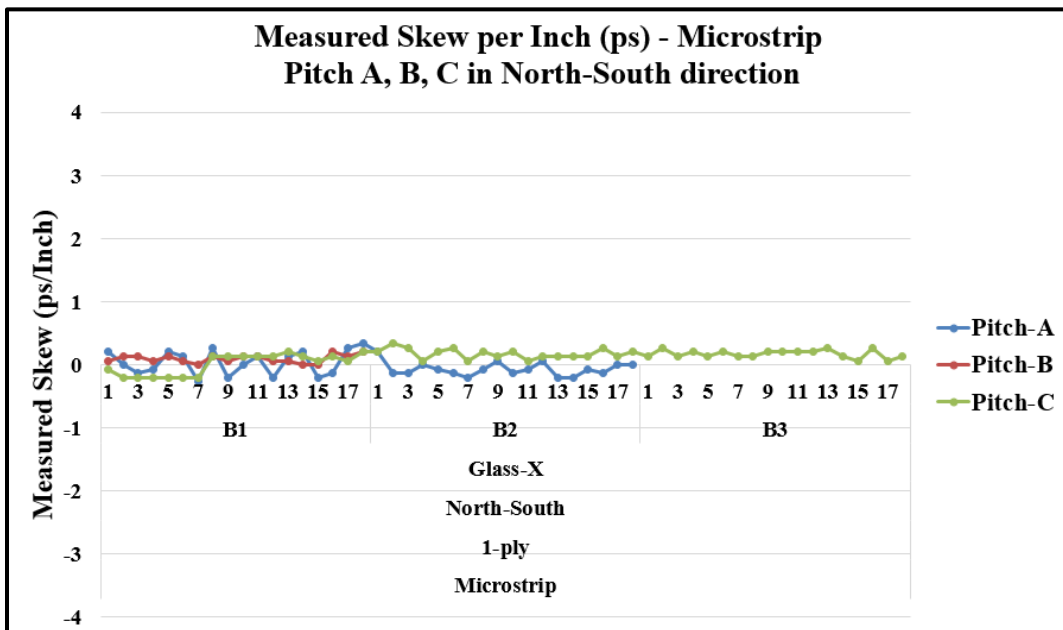


Figure 5.19. Skew on microstrip in North-South routing – Pitch A, B, C

5.3.2. Stripline – Pitch A, B, C. Skew comparison of pitch A, B, C stripline routing on 1-ply, glass X in West-East and North-South routing is shown in fig. 5.20 & 5.21. The measured worst case skew varies with the direction in which the traces are routed.

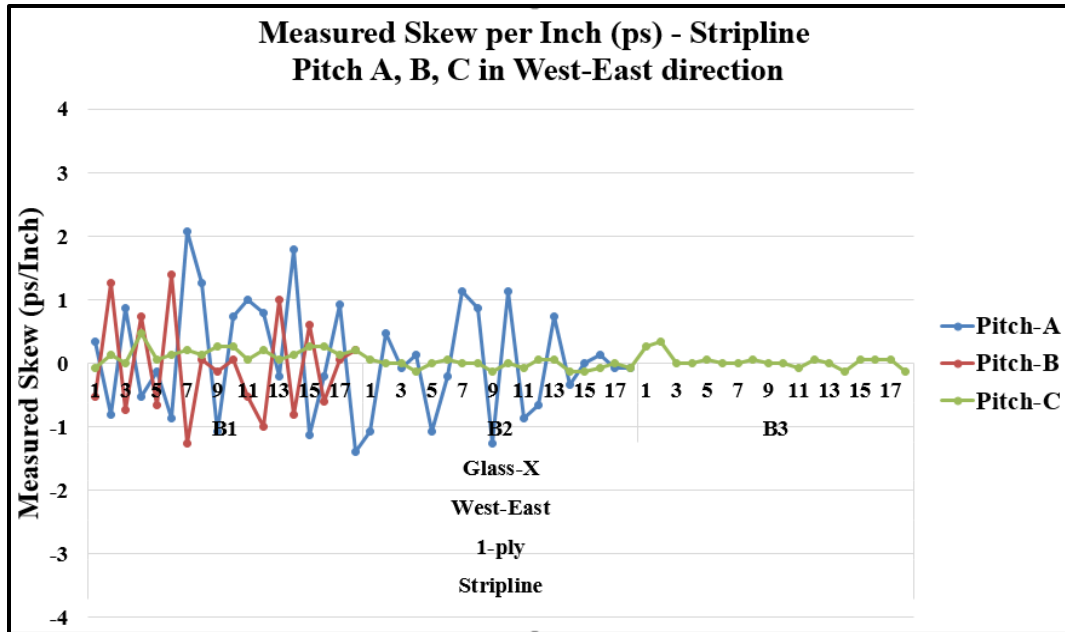


Figure 5.20. Skew on stripline in West-East routing – Pitch A, B, C

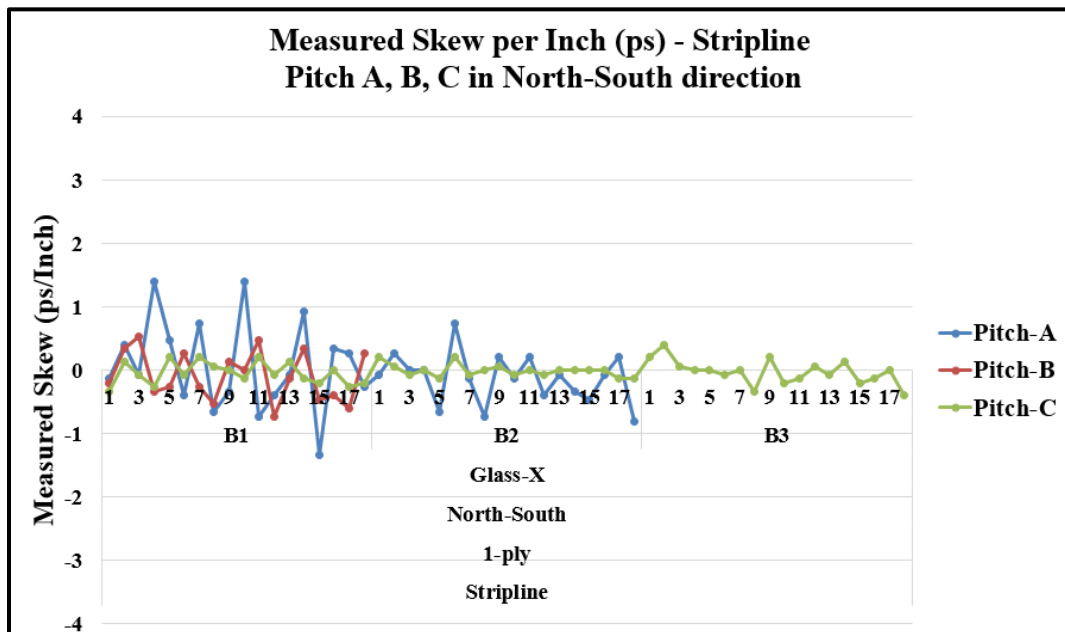


Figure 5.21. Skew on stripline in North-South routing – Pitch A, B, C

5.3.3. Stripline – Pitch A: Glass X vs. Y. Comparison of skew on glass X and Y routed in West-East, North-South directions on 1-ply, 2-ply glass styles is plotted in fig. 5.22 & 5.23. The maximum measured skew on glass Y is less than glass X.

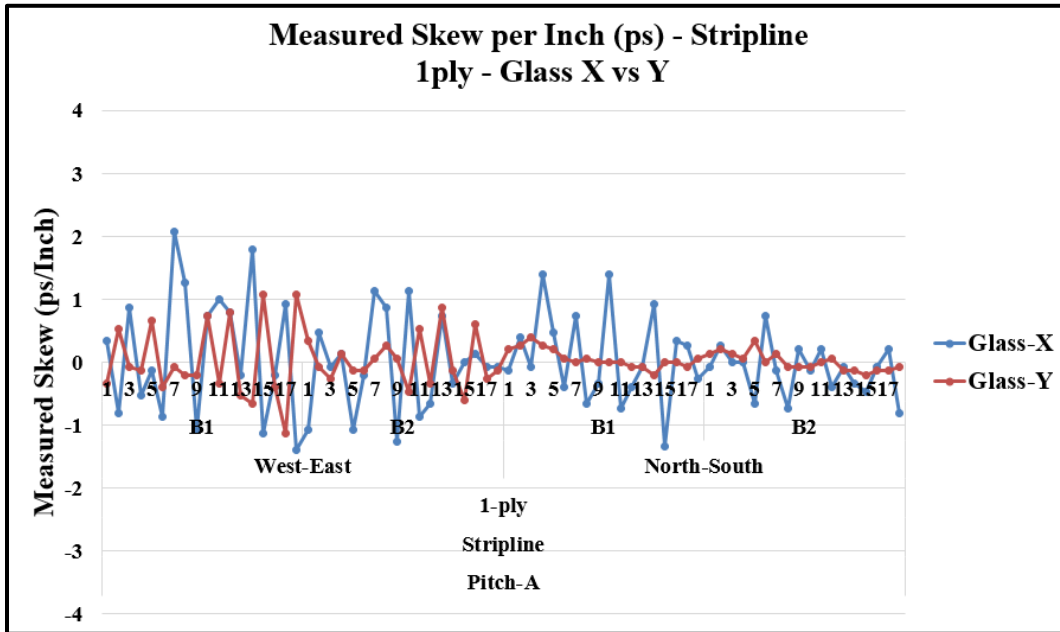


Figure 5.22. Skew on Pitch A, 1-ply glass style - Glass X vs Y

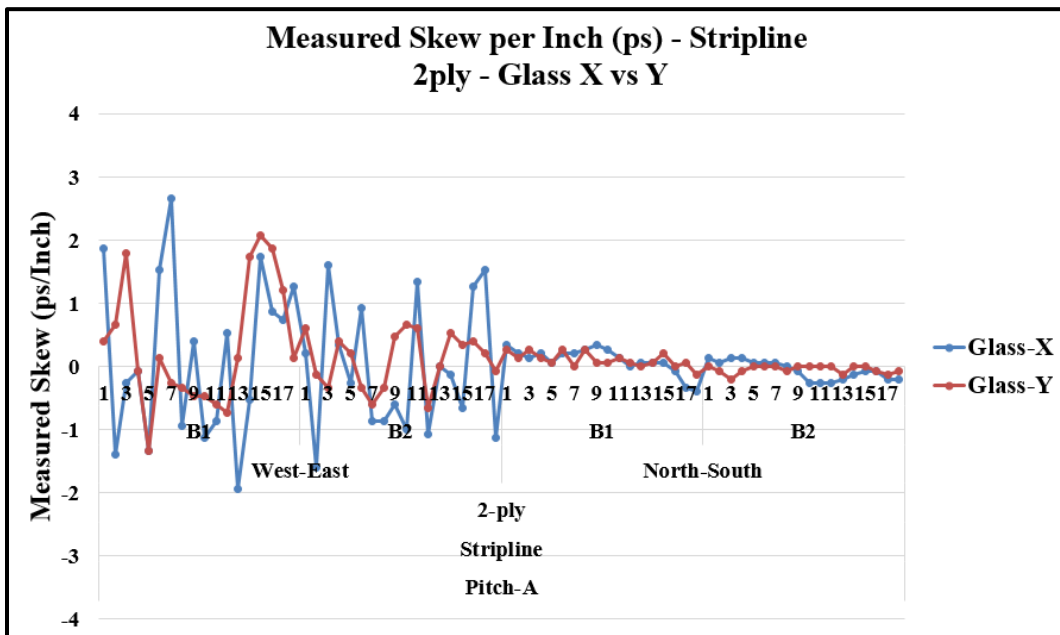


Figure 5.23. Skew on Pitch A, 2-ply glass style - Glass X vs Y

5.3.4. Stripline – Pitch C: Glass X vs. Y. Comparison of skew on glass X, Y in West-East, North-South direction on 1-ply and 2-ply glass is plotted in fig. 5.24 & fig. 5.25. The maximum measured skew on glass Y is slightly less than glass X.

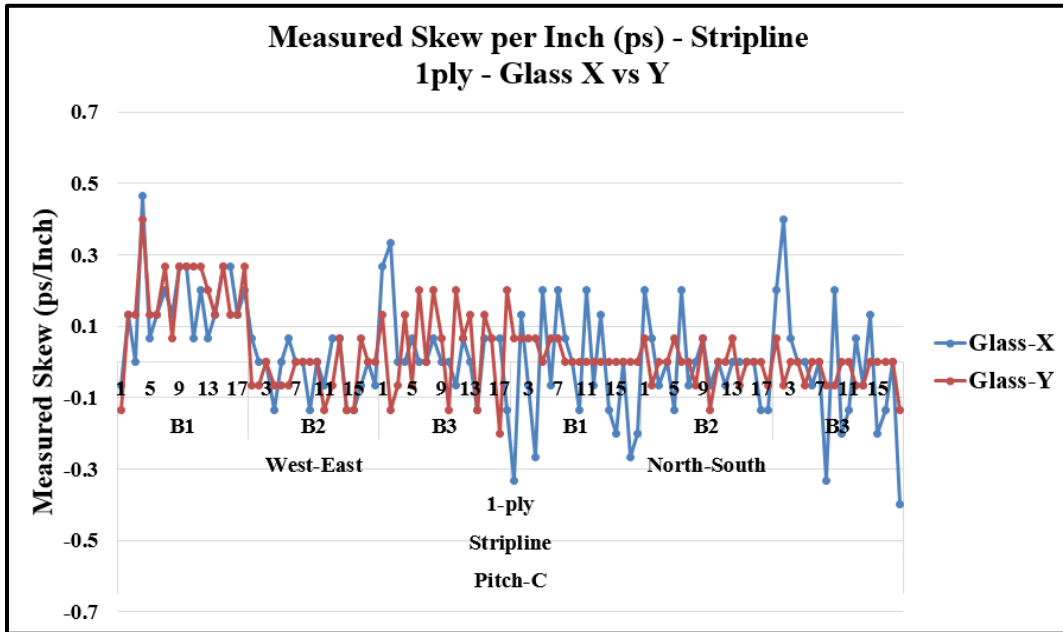


Figure 5.24. Skew on Pitch C, 1-ply glass style - Glass X vs Y

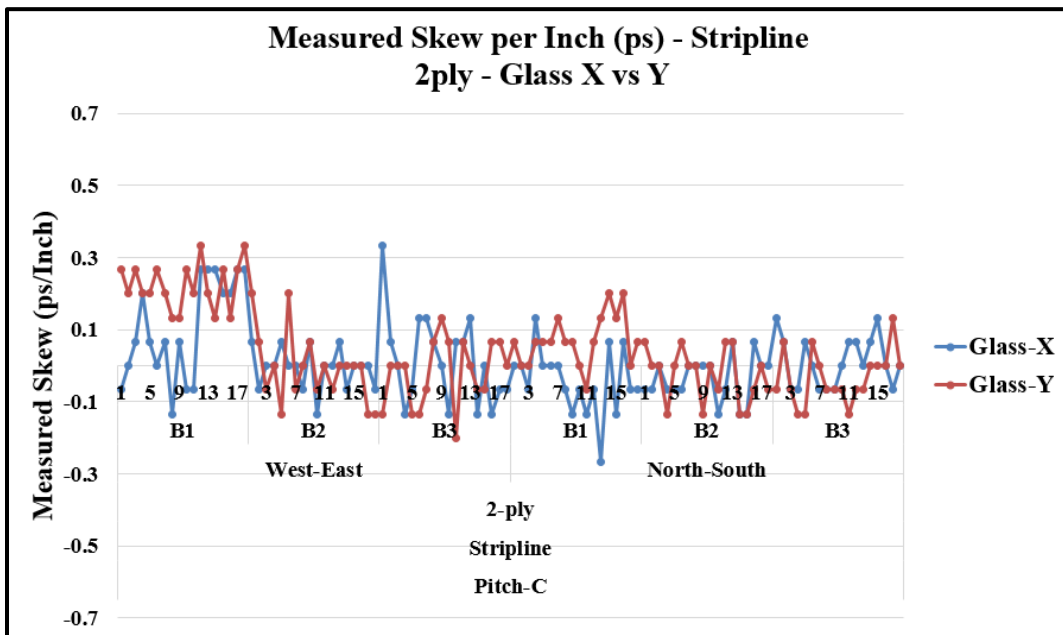


Figure 5.25. Skew on Pitch C, 2-ply glass style - Glass X vs Y

From measurement results shown in fig. 5.18 – 5.25, the worst case measured skew varies with glass material type, glass weave style, and the direction in which the traces are routed. In some cases, the maximum measured skew was 2ps/inch whereas in some other case, the maximum measured skew is below 0.5ps/inch. Hence by correct choice of glass style, glass material, direction of routing, glass weave skew can be bounded within 0.5ps/inch. The maximum skew measured on the boards is not the worst case skew as the bundle placement and trace locations with respect to the glass bundles cannot be controlled in fabrication. Therefore, simulation methodology along with measurement is necessary to make any solid conclusions.

6. FULL WAVE MODELING OF GLASS WEAVE

Few studies [15] performed earlier have modelled the fiber weave as a thick glass sheet with rectangular holes punched in it and resin fills the hole/gaps in the glass sheet. In some studies [4], [13] glass weave is modelled as 1D cascading of transmission lines with different propagation constants and characteristic impedances. In this work a full wave model [7] which accurately describes the spread glass instead of square glass is developed. Since the focus of this study to accurately find the worst case skew, full wave modeling is chosen although it comes at the cost of increased simulation time and computational resources.

6.1. MODELING STRIPLINE ON 1-PLY SPREAD GLASS

Full wave modeling of glass weave is done in HFSS. The dimensions and relative locations of the glass and traces cannot be known unless looked at the board cross-section. Hence the test vehicle is cut and pictures of PCB cross-section are obtained using SEM (Scanning Electron Microscope) as shown in fig. 6.1.

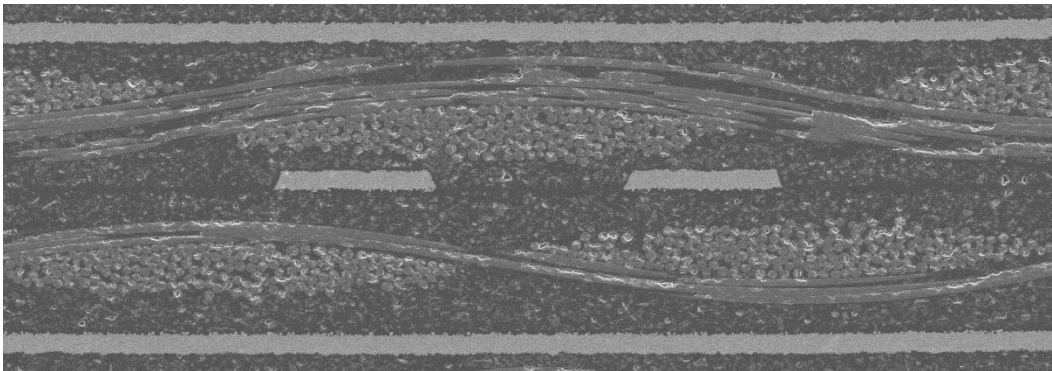


Figure 6.1. Cross-Section of a stripline obtained using SEM

The dimensions of the glass bundles, traces are calculated using Image tool in Matlab. The cross-section from SEM image is replicated in Ansys HFSS as in fig. 6.2 (top) & 6.2 (bottom). The glass bundles are modelled as ellipse swept along a sine curve. The simulation model is 102.9 mil long with 6 glass bundles along its length and width.

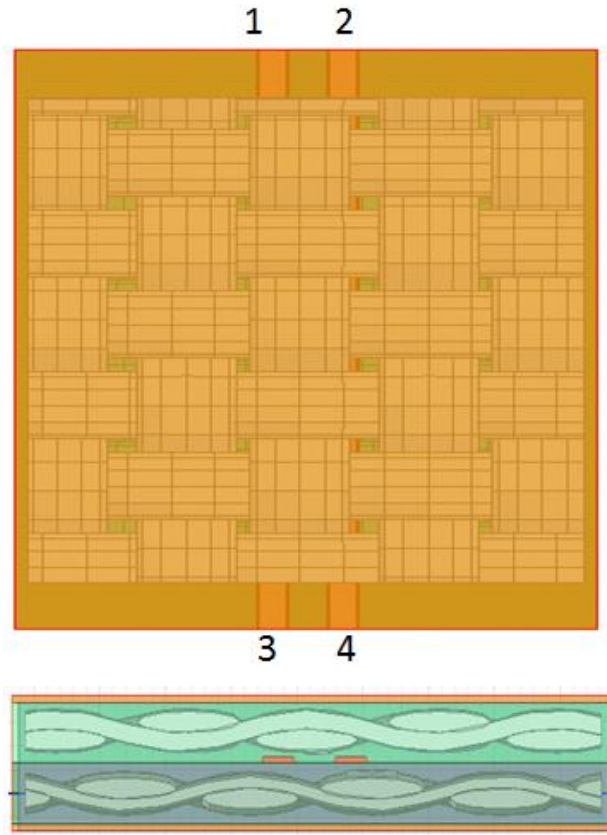


Figure 6.2. Full wave model of stripline embedded in glass weave fabric. Top View (Top), Cross-section view (Bottom)

Wave ports are used to excite the structure with TEM mode. The PCB cross-section is not uniform as the dielectric is a composite of glass and resin. Since the port should see uniform cross-section to excite a TEM mode, the traces are extruded outside the glass bundle region by 10 mils as shown in fig. 6.2 (top). The extruded portion is later de-embedded in HFSS. Adaptive meshing is done at 20 GHz solution frequency with maximum delta between consecutive passes being 0.001. Meshing should be dense where the currents or fields change rapidly. Hence, meshing on trace, ports, and glass bundles is increased by specifying the maximum mesh size constraint. Max mesh size on trace is set to 1mil, on port is set to 2 mils and inside the glass bundles is set to 2 mils. Radiation boundary condition is used on all sides. To reduce the simulation time, HPC (High power computing) with 6 cores is used.

To make sure that the S-Parameter accuracy is not lost when multiple S-Parameter blocks are cascaded, sanity check is performed to compare the S-Parameters from a 411.6 mils long full wave model shown in fig. 6.3 to the S-parameters obtained from cascading four S-parameter blocks of 102.9 mils long model as shown in fig.6.4.

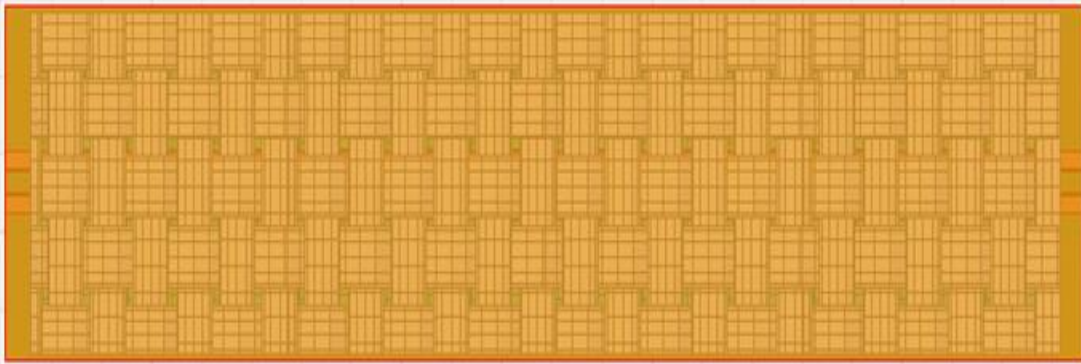


Figure 6.3. Full wave model of 411 mil long stripline embedded in glass weave fabric.

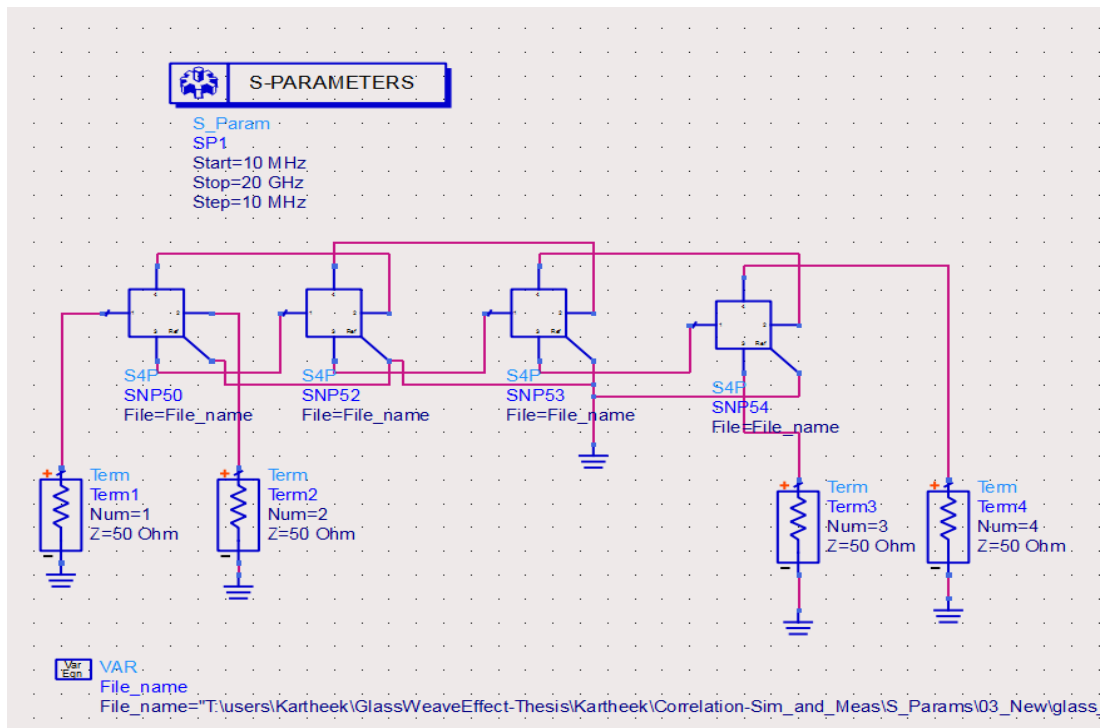


Figure 6.4. ADS circuit – Cascading (4 X 102.9 mil)

Return loss of full wave model and cascaded model are plotted in fig. 6.5 & insertion loss is plotted in fig 6.6.

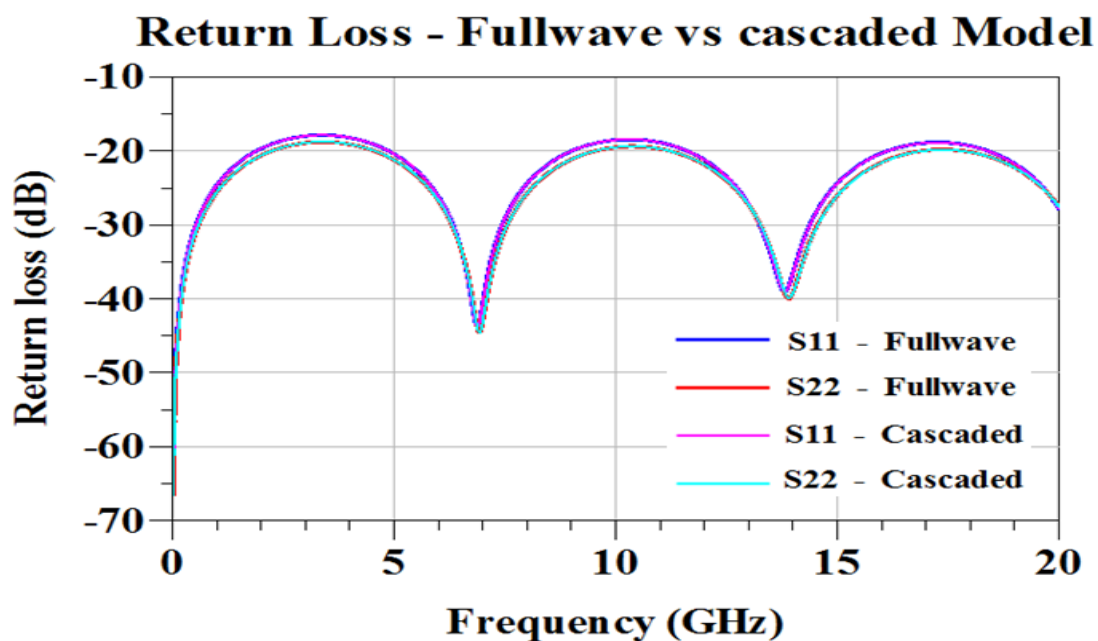


Figure 6.5. Return loss – Full wave vs Cascaded Model

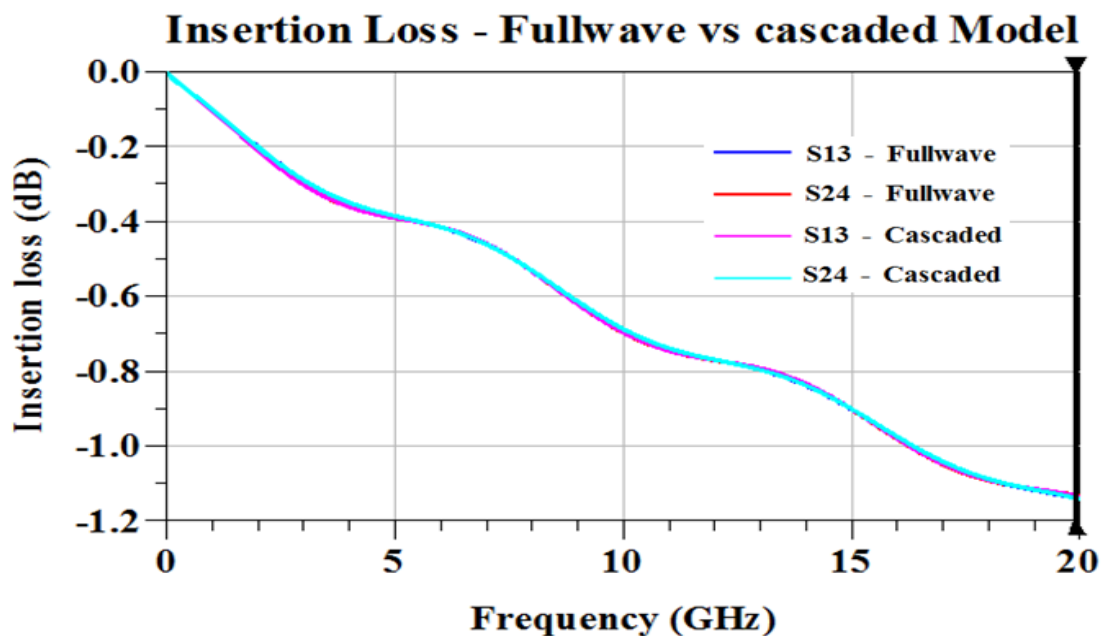


Figure 6.6. Insertion loss – Full wave vs Cascaded Model

Comparison of unwrapped phase of S_{13} and S_{24} between full wave model and cascaded model is shown in fig. 6.7.

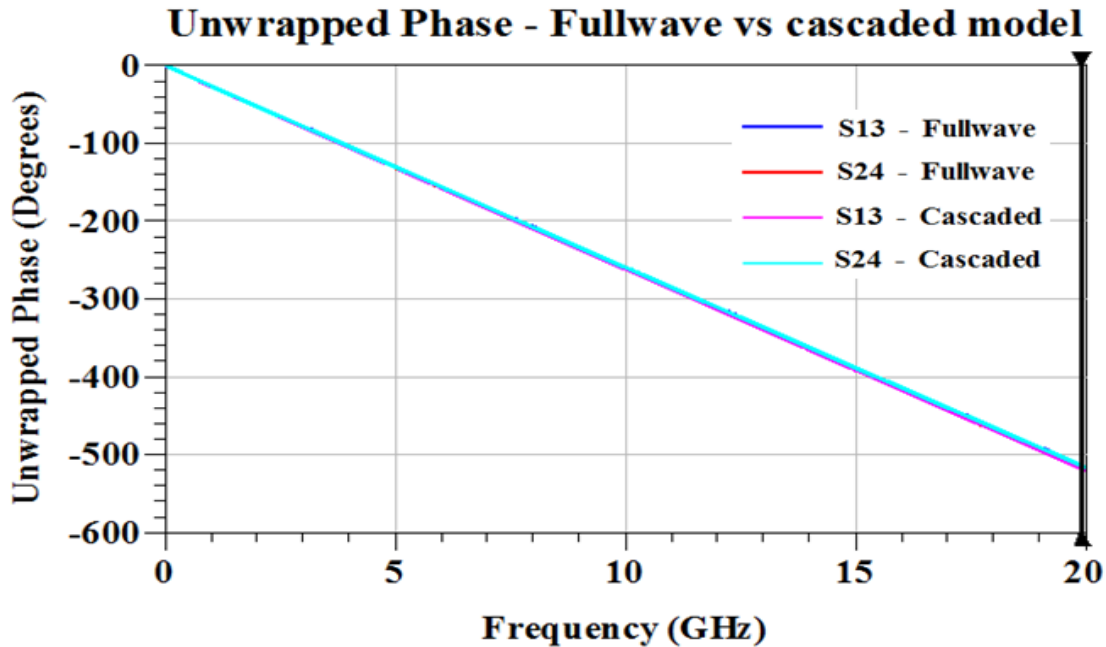


Figure 6.7. Unwrapped Phase – Full wave vs Cascaded Model

Insertion loss and unwrapped phase at one frequency (19.90 GHz) for full wave model and cascaded model is shown in table 6.1. The difference in magnitude is 0.001dB, 0.1° degree in phase. Since the difference in cascaded model and full wave model is very less, the s-parameters of 102.9 mils model can be cascaded to get s-parameters of a 15 inch long transmission line.

Table 6.1 Insertion loss and unwrapped phase @ 19.9 GHz

	dB (S13)	dB(S24)	Unwrapped phase(S13)	Unwrapped phase(S24)
Full Wave Model	-1.132 dB	- 1.140 dB	-517.659°	-514.144°
Cascaded Model	-1.133 dB	- 1.139 dB	-517.725°	-514.203°

6.2. VALIDATION OF SIMULATION MODEL

In simulation, s-parameters of 15 inch long line are obtained by cascading several s-parameter blocks of a smaller full wave simulation model (102.9 mils long). The dielectric constant (DK) and loss tangent (DF) of glass and resin in the full wave simulation model are tuned to get a good correlation to the measurement. The tuned DK, DF values of glass and resin are tabulated in table 6.2.

Table 6.2 DK, DF of Glass and Resin from Correlation

Material	DK	DF
Glass	6	0.0058
Resin	3.65	0.02

Unwrapped phase of S13, S24 are plotted in fig. 6.8 & fig. 6.9. Unwrapped Phase values of simulation and measurement at one frequency (19.68 GHz) are tabulated in table 6.3.

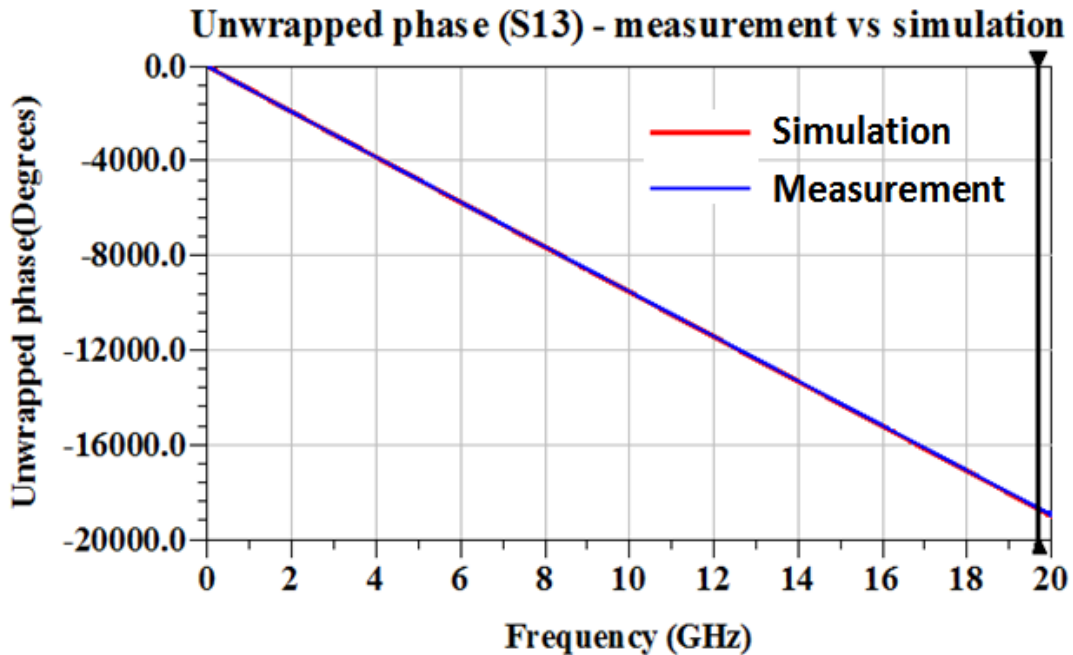


Figure 6.8. Unwrapped Phase (S13) – Simulation vs Measurement

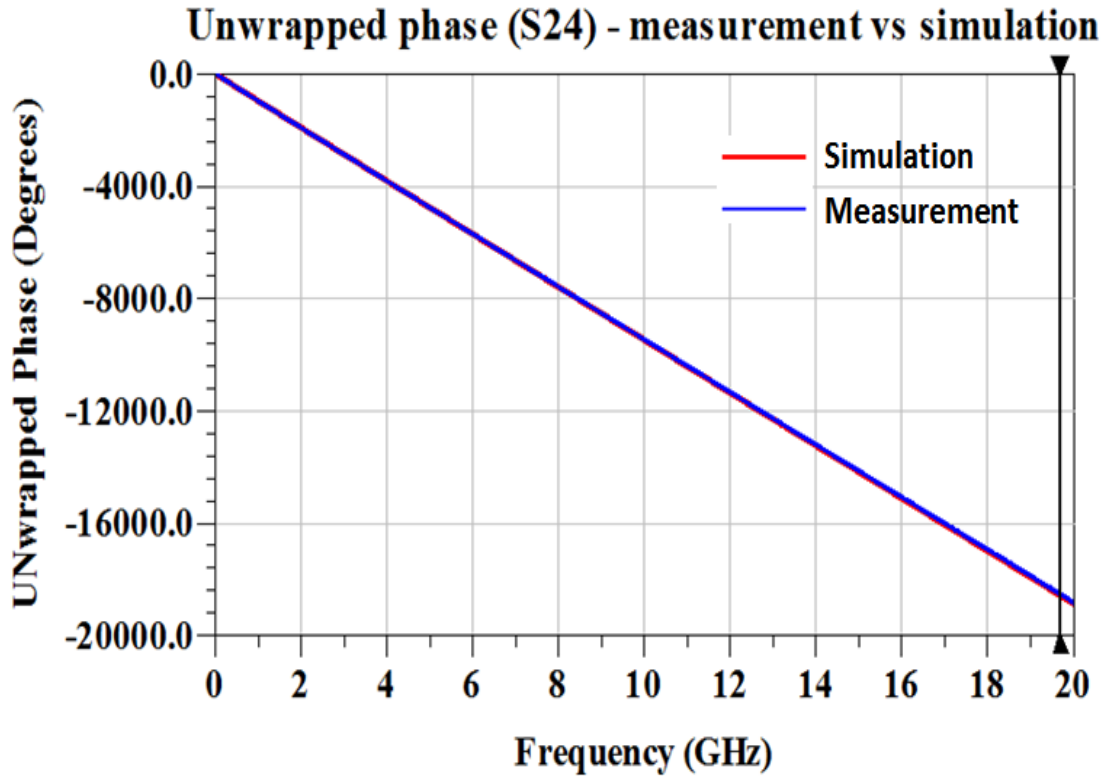


Figure 6.9. Unwrapped Phase (S24) – Simulation vs Measurement

Table 6.3 Unwrapped phase comparison between simulation and measurement

	Unwrapped phase (S13)	Unwrapped phase (S24)
Simulation	-18,705°	-18,562°
Measurement	-18,680°	-18,516°

From table 6.3, the phase difference in S_{13} and S_{24} between simulation and measurement is only 0.3% of the phase of simulation. Hence it can be treated as good correlation between simulation and measurement in terms of phase.

Magnitude comparison of S_{13} , S_{24} between simulation and measurement are plotted in fig. 6.10 & 6.11. It can be observed that the maximum difference in dB between simulation and measurement is less than 1 dB.

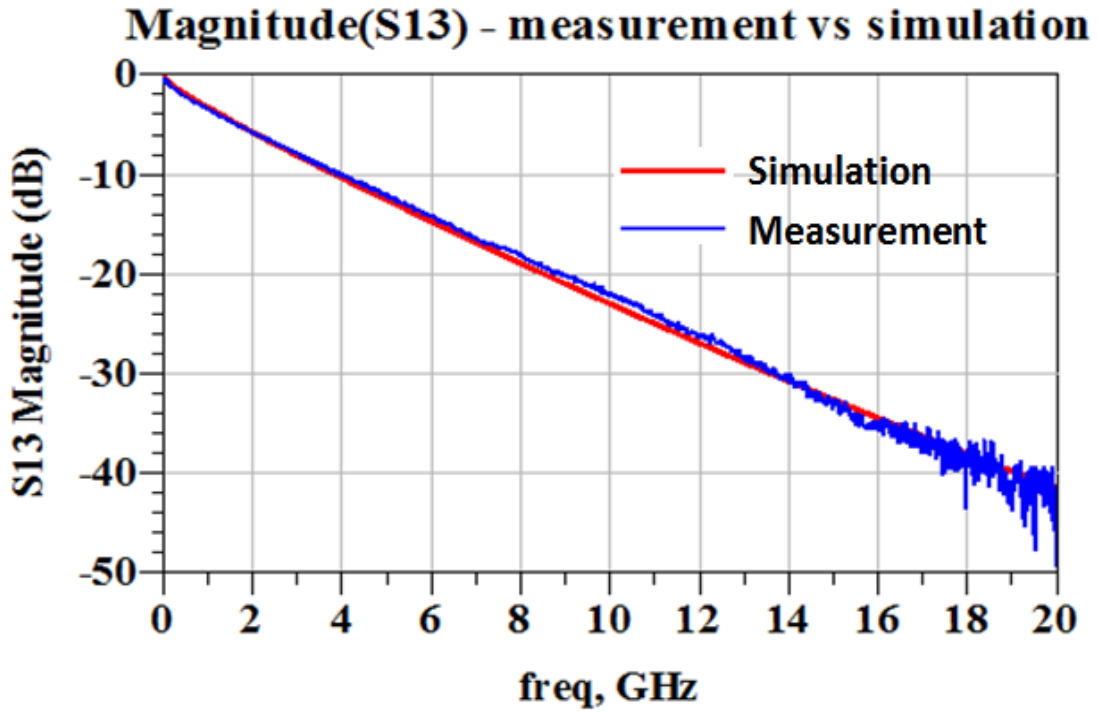


Figure 6.10. Magnitude (S13) – Simulation vs Measurement

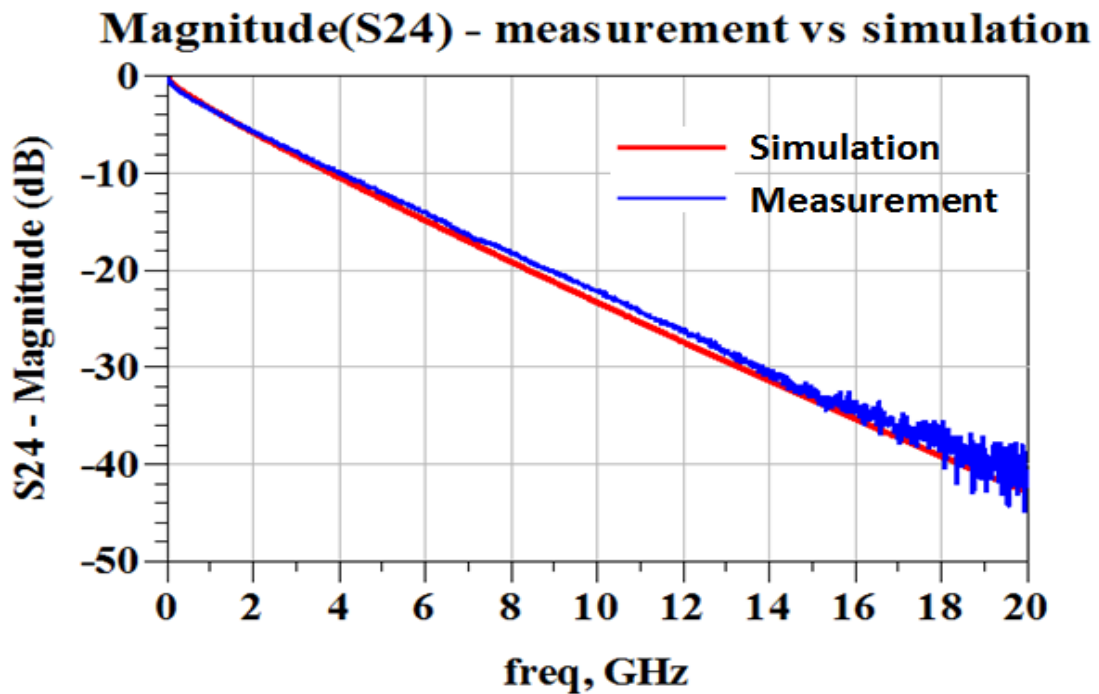


Figure 6.11. Magnitude (S24) – Simulation vs Measurement

As mentioned earlier, skew is calculated as difference in zero crossing times of TDT. TDT between ports 1, 3 is defined as TDT13. TDT between ports 2, 4 is defined as TDT24. TDT comparison between simulation and measurement is plotted in fig. 6.12.

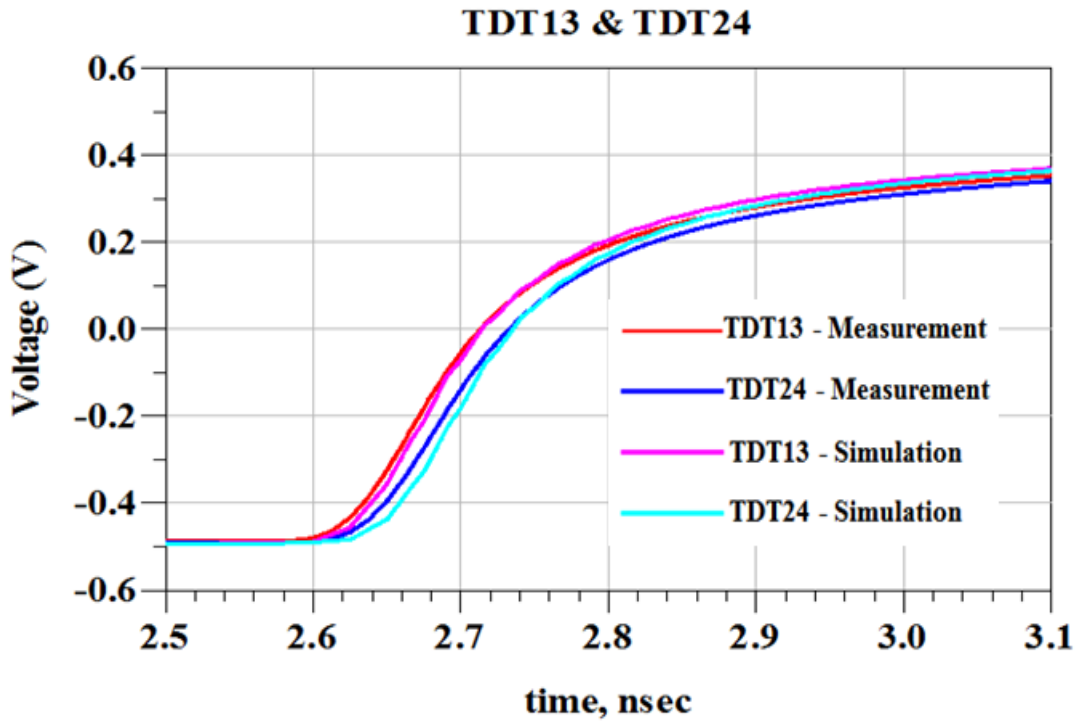


Figure 6.12. TDT – Simulation vs Measurement

Zero crossing time of TDT, skew of 15 inch trace, skew per inch are tabulated in table 6.4. The skew between simulation and measurement is matched within a margin of 0.2 ps/inch.

Table 6.4 TDT zero crossing times and skew – Simulation vs Measurement

	TDT24 (Zero Crossing)	TDT13 (Zero Crossing)	Skew (ps) (15 Inch)	Skew per Inch (ps)
Measured	2.733 ns	2.713 ns	20	1.281
Simulated	2.735 ns	2.714 ns	21	1.407

6.3. RESULTS AND DISCUSSION

6.3.1. Microstrip – Pitch A. A differential microstrip model as shown in fig. 6.13 is created similar to the stripline model and correlated DK, DF of glass and resin are used in this model. In simulation model, center to center distance between the traces is ‘A’ mils and the trace width and spacing is adjusted to get 100 Ohm differential impedance for pitch A model.

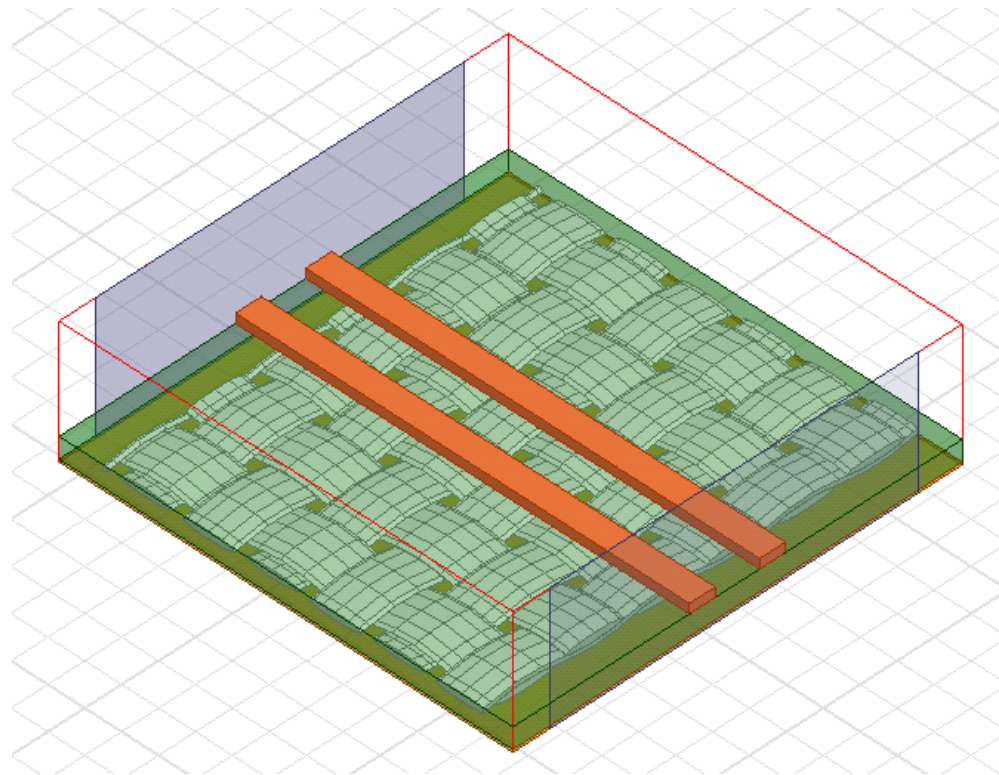


Figure 6.13. Full wave model of Microstrip

Pitch of glass bundle is divided into 10 steps and is used as step size for sweeping the location of differential trace with respect to glass bundles to complete one cycle from $n = 0$ to $n = 10$. Trace center is aligned with the center of glass bundle for $n = 0$ & $n = 10$. These models are simulated in HFSS and s-parameters are extracted. Skew is calculated using the methodology explained previously. The skew vs trace location is plotted in fig. 6.14. It is observed that the maximum simulated skew on pitch A is 4ps/inch whereas the maximum measured skew is 3ps/inch.

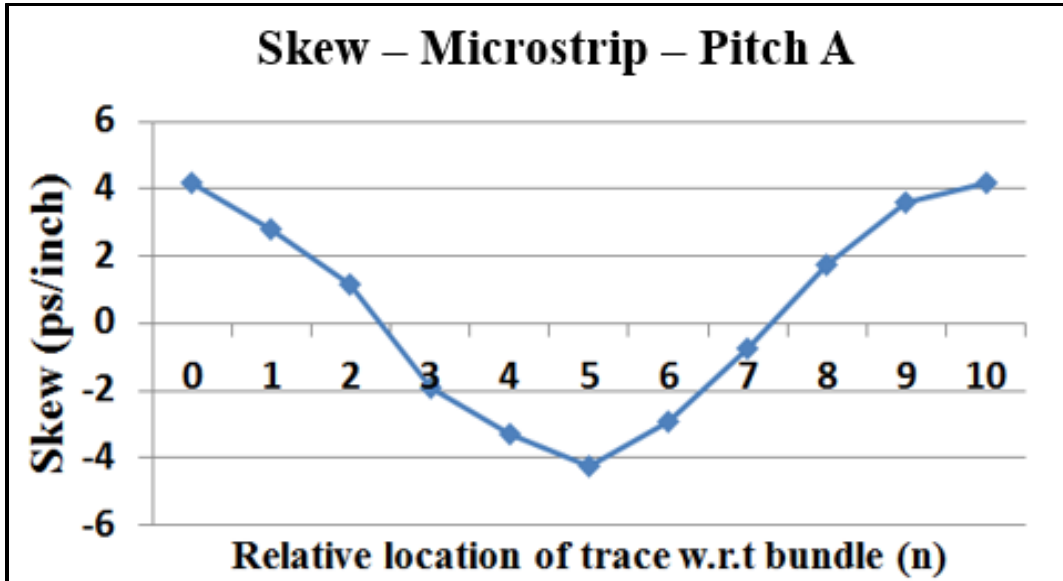


Figure 6.14. Microstrip – Pitch A – Skew vs trace location

6.3.2. Stripline – Pitch A. Similar to the trace sweep in microstrip case, the location of trace is shifted in 10 steps to complete one full cycle on pitch A stripline differential pair as shown in fig. 6.15.

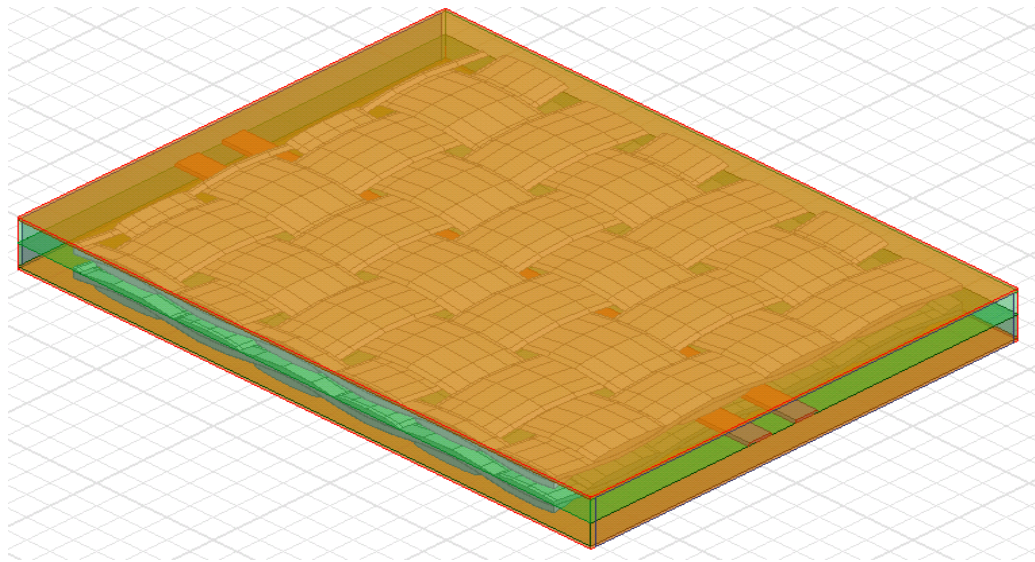


Figure 6.15. Stripline on 1-ply glass.

Skew vs trace location for pitch A, B and C is plotted in fig. 6.16. The worst case skew in 1-ply stripline case can be as high as 9ps/inch. Similar study can be performed using different glass materials and glass styles to quantify the worst case skew on them.

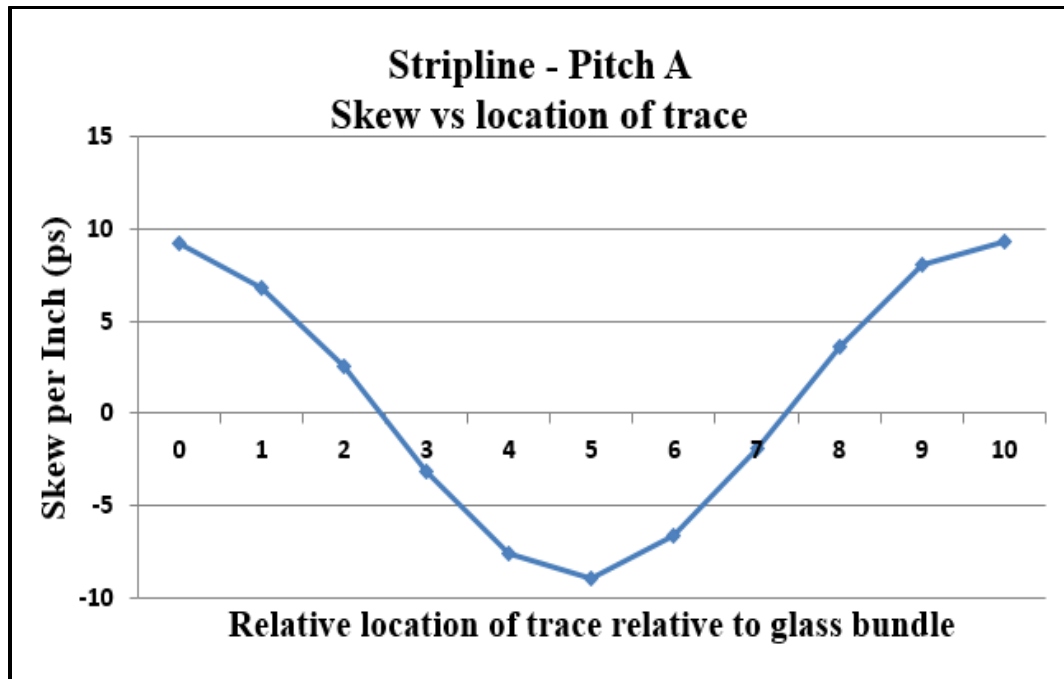


Figure 6.16. Skew vs location of trace – Pitch A

It is observed in the SEM pictures that bundle dimensions like bundle widths, bundle gaps, bundle pitch vary statistically. From limited number of SEM images, nominal and deviation of glass dimensions of 1-ply glass is calculated and is tabulated in table 6.5.

Table 6.5 Bundle dimensions from SEM in fill direction

Parameter	Dimensions from SEM	
	Nominal (mils)	Deviation (mils)
Fill width	15.36	0.62
Fill thickness	1.82	0.06

To evaluate the impact of the statistical variations on skew, simulation models with variations in glass dimensions have to be developed and studied. Due to many variables like glass thickness, width, thickness, trace thickness, trace pitch, dielectric height, etc., the number of variations can be very large.

6.3.3. Methodology to Obtain the Worst Case Skew. As the relative location of traces with respect to glass bundles varies statistically, the probability to hit the worst case skew from limited measurements on test vehicles, a methodology using measurements and full wave simulations is employed. Methodology can be summarized in flow chart as shown in fig. 6.17

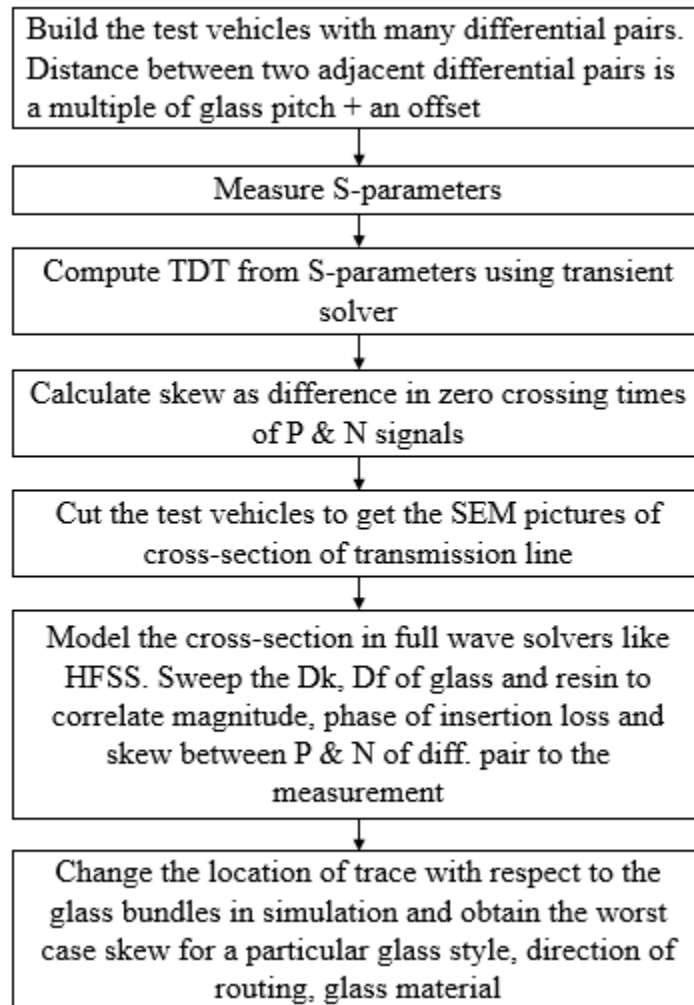


Figure 6.17. Methodology to capture the worst case skew on a particular glass

The process can be repeated with different glass weave styles, direction of routing, glass materials like standard glass, low Dk glass, multiple ply dielectrics to obtain the worst case skew in each case and make design decisions based on the worst case skew numbers

7. CONCLUSION AND FUTURE WORK

Mitigation of glass weave skew using a combination of low DK spread glass, laminate with multiple ply glass and routing direction is studied in this thesis. A measurement and simulation methodology to mitigate the worst case skew is presented in this work. Some conclusions from this work are

- Worst case skew on microstrip differential pair can be as high as 4 ps/inch.
- Worst case skew on stripline differential pair can be as high as 9ps/inch.
- The worst case skew on microstrip and stripline differential pairs can be bounded to below 0.5 ps/inch by using a combination of low DK glass material, glass weave style, multi-ply dielectrics and the routing direction.

The simulation methodology can be applied to quantify the reduction in the worst case skew on low DK glass when compared to standard glass. A more robust way of analyzing the effect of manufacturing variations on skew using design of experiments need to be developed.

BIBLIOGRAPHY

- [1] X. Tian et al., "Numerical investigation of glass-weave effects on high-speed interconnects in printed circuit board," 2014 IEEE International Symposium on Electromagnetic Compatibility (EMC), Raleigh, NC, 2014, pp. 475-479.
- [2] S. McMorro, C. Heard, "The Impact of PCB Laminate Weave on the Electrical Performance of Differential Signaling at Multi-Gigabit Data Rates," DesignCon 2005.
- [3] J. Miller, G. Blando, I. Novak, "Additional Trace Losses due to Glass-Weave Periodic Loading," DesignCon 2010.
- [4] P. Pathmanathan, P. Huray, S. Pytel, "Analytic Solutions for Periodically Loaded Transmission Line Modeling," DesignCon 2013.
- [5] J. Loyer, R. Kunze, X. Ye, "Fiber Weave Effect: Practical Impact Analysis and Mitigation Strategies," White paper, Circuit tree.
- [6] Y. Shlepnev and C. Nwachukwu, "Modelling jitter induced by fibre weave effect in PCB dielectrics," 2014 IEEE International Symposium on Electromagnetic Compatibility (EMC), Raleigh, NC, 2014, pp. 803-808.
- [7] C. Herrick, T. Buck, R. Ding, "Bounding the Effect of Glass Weave through Simulation," DesignCon 2009.
- [8] A. Morgan, "Developments in Glass Yarns and Fabric Constructions," The PCB Magazine, March 2004.
- [9] "PCB Dielectric Material Selection and Fiber Weave Effect on High-Speed Channel Routing," Application Note, Altera.
- [10] https://en.wikipedia.org/wiki/Warp_and_woof, 13 July 2016.
- [11] Howard Heck, Steve Hall, Bryce Horine, Tao Liang; "Modeling and Mitigating AC Common Mode Conversion in Multi-Gb/s Differential Printed Circuit Boards"; DTTC 2004 Paper.
- [12] G. R. Luevano, J. Shin and T. Michalka, "Practical investigations of fiber weave effects on high-speed interfaces," 2013 IEEE 63rd Electronic Components and Technology Conference, Las Vegas, NV, 2013, pp. 2041-2045.
- [13] T. Zhang, X. Chen, J. E. Schutt-Ainé and A. C. Cangellaris, "Statistical analysis of fiber weave effect over differential microstrips on printed circuit boards," Signal and Power Integrity (SPI), 2014 IEEE 18th Workshop on, Ghent, 2014, pp. 1-4.

- [14] D. Bucur, "Fiber Weave Effect - a performance-limiting factor," Communications (COMM), 2014 10th International Conference on, Bucharest, 2014, pp. 1-4.
- [15] S. Singh and T. Kukal, "Timing skew enabler induced by fiber weave effect in high speed HDMI channel by angle routing technique in 3DFEM," Electrical Performance of Electronic Packaging and Systems (EPEPS), 2015 IEEE 24th, San Jose, CA, 2015, pp. 163-166.
- [16] M. Chernobryvko, D. V. Ginste and D. De Zutter, "A perturbation technique to analyze the influence of fiber weave effects on differential signaling," 2013 IEEE 22nd Conference on Electrical Performance of Electronic Packaging and Systems, San Jose, CA.
- [17] A. C. Durgun and K. Aygün, "Impact of fiber weaves on 56 Gbps SerDes interface in glass epoxy packages," Electrical Performance of Electronic Packaging and Systems (EPEPS), 2015 IEEE 24th, San Jose, CA, 2015, pp. 159-162.
- [18] Y. Cao, J. Li, J. Hu, M. Zheng and B. Li, "Design Consideration for 10 Gbps Signal Transmission Channel in Copper Backplane System," Computational Science and Its Applications (ICCSA), 2011 International Conference on, Santander, 2011, pp. 215-218.
- [19] A. Chada, B. Mutnury, J. Fan and J. L. Drewniak, "Crosstalk Impact of Periodic-Coupled Routing on Eye Opening of High-Speed Links in PCBs," in IEEE Transactions on Electromagnetic Compatibility, vol. 57, no. 6, pp. 1676-1689, Dec. 2015.
- [20] T. Fukumori, H. Nagaoka, D. Mizutani and M. Tani, "Simulation of differential skew considering fiber kink effects," IEEE CPMT Symposium Japan 2014, Kyoto, 2014, pp. 43-46.

VITA

Kartheek Nalla was born in Hyderabad, India in 1990. He obtained his Bachelor of Technology degree in Electronics and Communications Engineering from Jawaharlal Nehru Technological University (JNTU), Hyderabad in May 2011. He worked as a Systems Engineer in Infosys Ltd for over two years from October 2011 to December 2013. He was a master's student in the department of Electrical Engineering in Missouri University of Science and Technology from January 2014 and a graduate research assistant at EMC laboratory under Dr. Jun Fan, until he received his Master of Science degree in December 2016. He worked as intern at Cisco Systems Inc. between May 2015 – May 2016.